December 19, 2025

NOAA Chesapeake, Maryland

Shoreline Mapping Projects: MD2401-TB-C

Technical Data Report, NOAA Contract 1305M220DNCNL0064, Task Order 1305M224F0373

Prepared For:

National Oceanic and Atmospheric Administration
Stephen White
N/NGS3; SSMC-3 Sta. 8245
1315 East West Highway
Silver Spring, MD 20910

Prepared By:

NV5 Corvallis
1100 NE Circle Blvd, Ste. 126
Corvallis, OR 97330
PH: 541-752-1204

Table of Contents

Cover Photo: A view looking southwest from Long Point to Harbor Cove in Chesapeake Bay. The image was created from the lidar bare earth model colored by elevation.

List of Figures

List of Tables

INTRODUCTION

This photo, taken by NV5 acquisition staff, shows a view of the Chesapeake Bay within the project site in Maryland.

In August 2024, NV5 was contracted by National Oceanic and Atmospheric Administration (NOAA) to collect topobathymetric Light Detection and Ranging (lidar) data and digital imagery in the fall of 2024 for the NOAA Chesapeake site in Maryland. The NOAA Chesapeake area of interest stretched along the eastern shoreline of the Chesapeake Bay north from Tolchester to south near Cook Point Sanctuary. Traditional near-infrared (NIR) lidar was fully integrated with green wavelength lidar return data (bathymetric) in order to provide a seamless topobathymetric lidar dataset. Data were collected to aid NOAA in assessing the channel morphology and topobathymetric surface of the study area to support nautical charting and shoreline mapping to define America's marine territorial limits and manage coastal resources.

This report accompanies the delivered topobathymetric lidar data and documents contract specifications, data acquisition procedures, processing methods, and analysis of the final dataset including lidar accuracy, and density. Acquisition dates and acreage are shown in Table 1, a complete list of contracted deliverables provided to NOAA is shown in Table 3 with the coordinate reference system information for these deliverables shown in Table 2, and the project extent is shown in Figure 1.

Table 1: Acquisition dates, acreage, and data types collected on the NOAA Chesapeake site

Project Site	Contracted Acres	Contracted sq. miles	Buffered Acres	Buffered sq. miles	Aerial Acquisition Dates	Data Type
NOAA Chesapeake, Maryland	222,592	347.8	233,759	365.2	*11/9/2024 – 11/19/2024	Topobathymetric – Lidar

*See Figure 5 for more detailed flight dates for lidar acquisition

Deliverable Products

Table 2: Deliverable product coordinate reference system information

Deliverable	Projection	Horizontal Datum	Vertical Datum	Units
Classified LAZ	UTM Zone 18 North	NAD83(2011)	GRS80 (Ellipsoidal Height)	Meters
Raster Model	UTM Zone 18 North	NAD83(2011)	NAVD88(GEOID18)	Meters

Table 3: Lidar products delivered for the NOAA Chesapeake site

Product Type	File Type	Product Details
Points	LAZ v.1.4 (*.laz), Point Format 6	• All Unclassified Returns
Rasters	1.0-meter, 5000 x 5000 m tiled Cloud Optimized GeoTIFFs (*.tif)	• Bathymetric Void-Clipped Topobathymetric Bare Earth Digital Elevation Model (DEM) • Normalized Seabed Intensity Rasters • Pilot Delivery Green Laser DZ Orthos • Pilot Delivery NIR Laser DZ Orthos • Pilot Delivery Topobathymetric Standard Deviation Model
Vectors	Shapefiles (*.shp)	• Buffered Project Boundary • 500 x 500 m Lidar Tile Index • 5000 x 5000 m DEM Tile Index • Aerial Acquisition Shapes (Lidar Flightlines and Lidar Flightline Swaths) • Ground Survey Data • Bathymetric Void Shape • Feedback Edits with Response
Flightline & Sensor Trajectories	Trajectories (*.txt)	• Chiroptera 4X
TPU Products	1.0-meter, 5000 x 5000 m tiled GeoTIFFs (*.tif)	• 2-band Total Propagated Uncertainty (TPU) Raster Model ○ Band 1 Total Horizontal Uncertainty (THU) at 95% Confidence ○ Band 2 Total Vertical Uncertainty (TVU) at 95% Confidence
Metadata	Extensible Markup Language (*.xml)	• LAS Metadata • Bare Earth DEM Metadata • TPU Raster Metadata • Normalized Intensity Metadata • Project Boundary Metadata • LAS Index Metadata • DEM Index Metadata • Bathymetric Void Shape • Feedback Edits with Response
Reports	Adobe Acrobat (*.pdf)	• Field Data Collection Sheets • Ground Survey Report • Lidar Boresight Calibration Reports • Lidar Technical Data Report

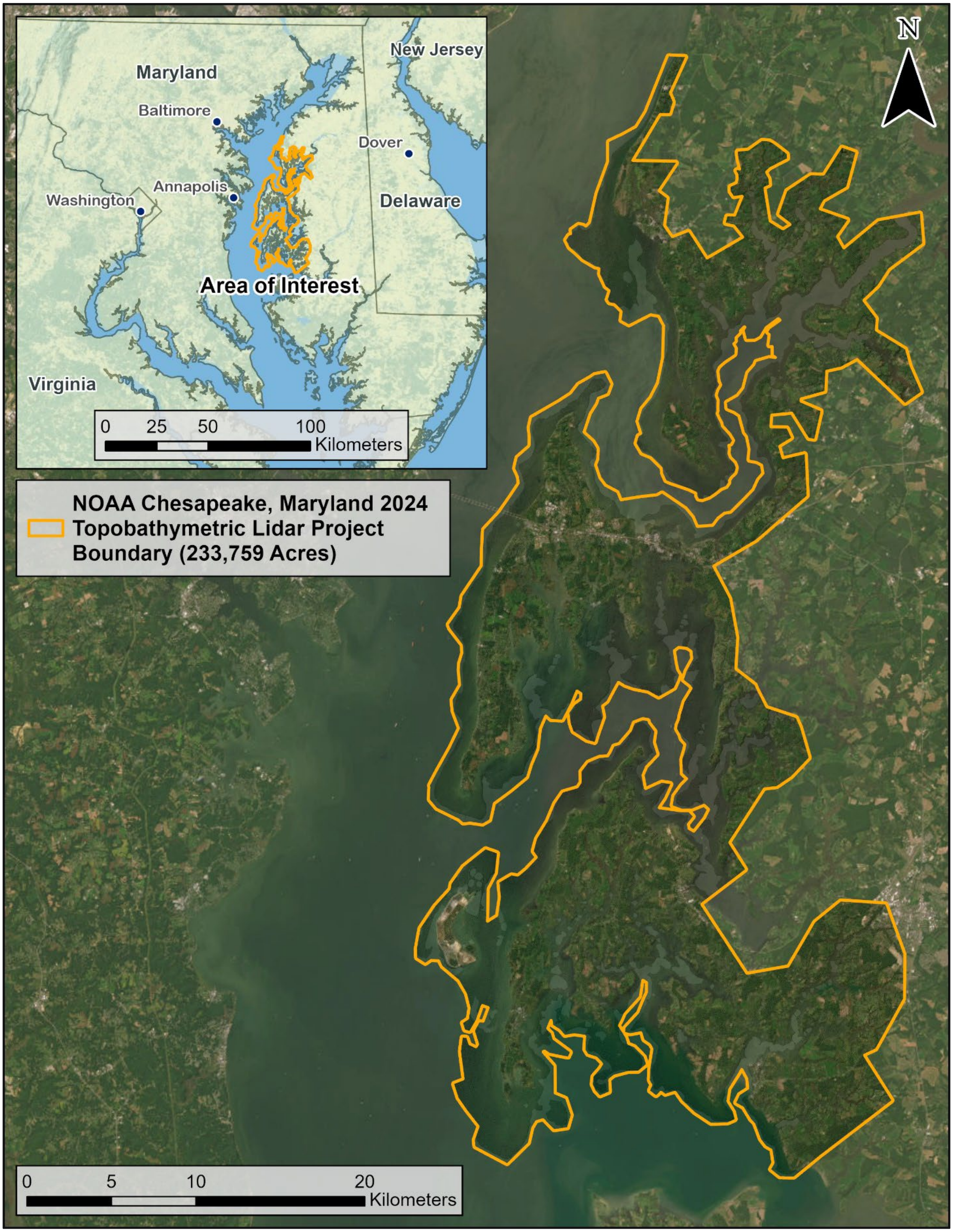

Figure 1: Location map of the NOAA Chesapeake site in Maryland

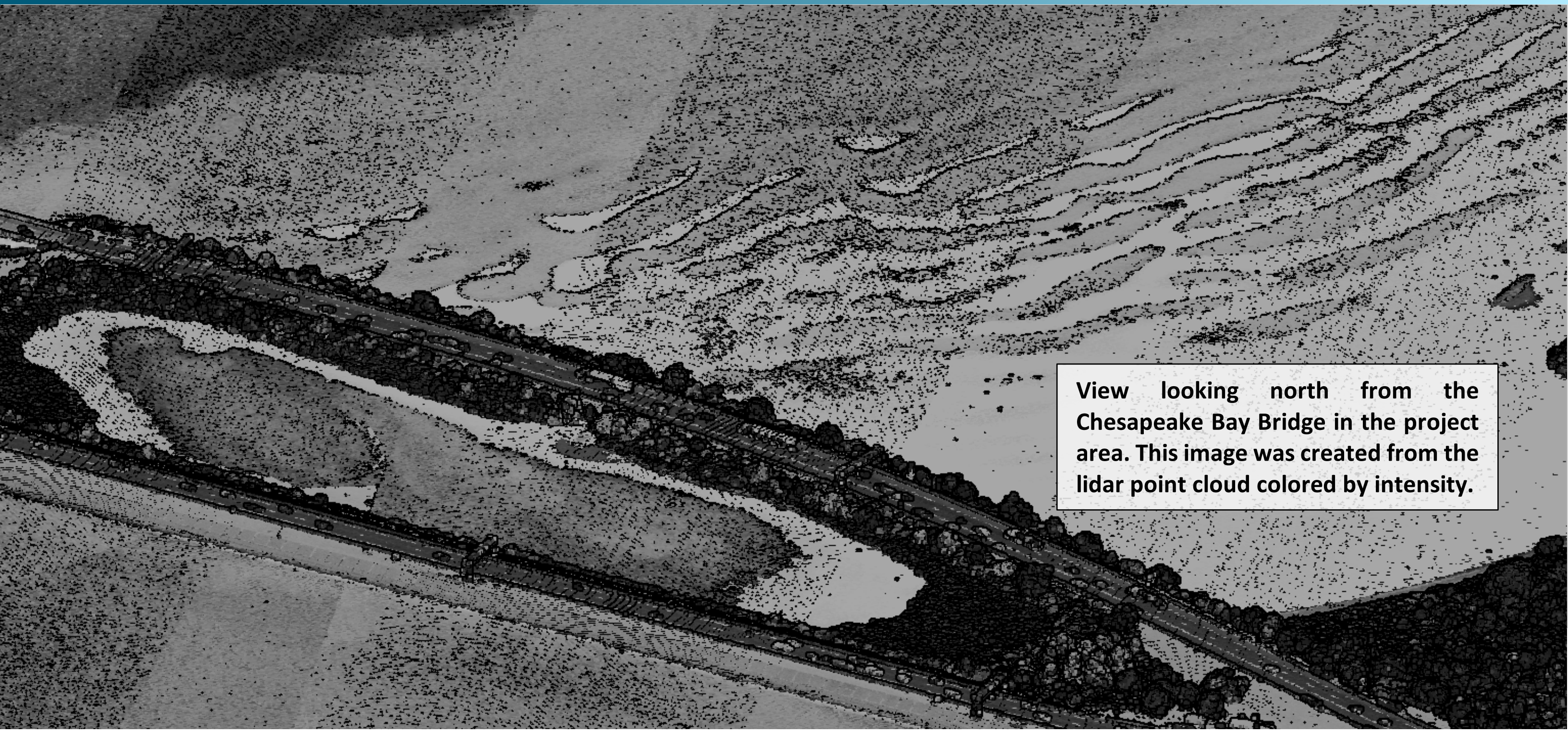

View looking north from the Chesapeake Bay Bridge in the project area. This image was created from the lidar point cloud colored by intensity.

Planning

In preparation for data collection, NV5 reviewed the project area and developed a specialized flight plan to ensure complete coverage of the NOAA Chesapeake lidar study area at the target combined point density of at least 3 points/m^2 for bathymetric returns and at least 4 points/m^2 for NIR returns. Acquisition parameters including orientation relative to terrain, flight altitude, pulse rate, scan angle, and ground speed were adapted to optimize flight paths and flight times while meeting all contract specifications. Figure 5 shows these optimized flight paths and dates.

Factors such as satellite constellation availability and weather windows must be considered during the planning stage. Any weather hazards or conditions affecting the flight were continuously monitored due to their potential impact on the daily success of airborne and ground operations. In addition, logistical considerations including private property access, potential air space restrictions, tide conditions and surface elevation (Figure 2 and Figure 3), and water clarity (Figure 4) were reviewed.

Turbidity Measurements and Secchi Depth Readings

In order to assess water clarity conditions prior to and during lidar and digital imagery collection, NV5 collected turbidity measurements, Secchi depth readings, and wind speed and direction measurements. Readings were collected at 16 locations throughout the project site from November 9th to 17th, 2024. Turbidity observations were recorded three times to confirm measurements. Table 4 below provides turbidity and Secchi depth results per site on each day of data collection. A true Secchi depth reading is where the Secchi depth reaches extinction. However, because of safety concerns and accessibility, some Secchi depth readings were noted to have reached the bottom surface of the riverbed.

Table 4: 2024 Water clarity observations for lidar flights

Date	Time (UTC - 4)	Location	Latitude	Longitude	Turbidity Read 1 (NTU)	Turbidity Read 2 (NTU)	Turbidity Read 3 (NTU)	Secchi Depth (cm)	Wind Speed (knots)
11/9	11:50 am	Site 001: North side of pier at “Doc’s Sunset Grill”	38° 40' 59.73293" N	76° 10' 23.27135" W	6.48	5.98	6.00	*152	7-10.2, from NW
11/9	7:00 pm	Site 001: North side of pier at *Doc’s Sunset Grill*	38° 40' 59.73293" N	76° 10' 23.27135" W	5.83	5.59	5.36	*121	2.4-2.7, from NW
11/12	9:35 am	Site 001: North side of pier at “Doc’s Sunset Grill”	38° 40' 59.73293" N	76° 10' 23.27135" W	5.12	6.23	5.55	120	10-11.1, from NW
11/11	3:38 pm	Site 002: Dogwood Harbor	38° 42' 43.94901" N	76° 20' 05.12386" W	8.85	9.56	10.1	77	4.5-5.0, from SW
11/11	2:55 pm	Site 003: Clairborne Landing	38° 50' 13.83178" N	76° 16' 50.43062" W	4.19	4.05	4.42	*78	6.2, from SW
11/11	4:45 pm	Site 003: Clairborne Landing	38° 50' 13.83178" N	76° 16' 50.43062" W	3.78	4.80	4.88	*72	0
11/7	2:20 pm	Site 004: Kent Point Marina	38° 50' 14.61397" N	76° 22' 25.68581" W	3.67	6.79	3.76	N/A	0
11/10	2:12 pm	Site 004: Kent Point Marina	38° 50' 14.61397" N	76° 22' 25.68581" W	5.73	5.43	6.37	*75	9.1-10.3, from SE
11/17	11:08 am	Site 004: Kent Point Marina	38° 50' 14.61397" N	76° 22' 25.68581" W	4.40	5.41	5.67	84	3, from WNW
11/17	1:46 pm	Site 004: Kent Point Marina	38° 50' 14.61397" N	76° 22' 25.68581" W	4.32	3.28	3.34	86	<1
11/18	11:39 am	Site 004: Kent Point Marina	38° 50' 14.61397" N	76° 22' 25.68581" W	2.78	3.08	3.12	72	2.4, from NW

Date	Time (UTC - 4)	Location	Latitude	Longitude	Turbidity Read 1 (NTU)	Turbidity Read 2 (NTU)	Turbidity Read 3 (NTU)	Secchi Depth (cm)	Wind Speed (knots)
11/10	4:56 pm	Site 005: Crab Alley Marina	38° 56' 09.24088" N	76° 17' 09.21721" W	4.07	4.55	5.57	*79	8.0-9.2, from S
11/15	12:06 pm	Site 005: Little Creek Public Landing	38° 56' 09.24088" N	76° 17' 09.21721" W	2.94	3.18	3.25	*167	5.0-7.0, from WNW
11/16	10:35 am	Site 005: Little Creek Public Landing	38° 56' 09.24088" N	76° 17' 09.21721" W	3.32	4.04	3.66	*130	13-18.4, from WNW
11/16	12:20 pm	Site 005: Little Creek Public Landing	38° 56' 09.24088" N	76° 17' 09.21721" W	4.10	3.64	3.79	58	5.8-11.0, from SW
11/17	10:29 am	Site 006: Libbey's Coastal Kitchen and Cocktails	38° 58' 48.43966" N	76° 20' 04.14930" W	3.66	3.44	3.31	140	0
11/17	1:19 pm	Site 006: Libbey's Coastal Kitchen and Cocktails	38° 58' 48.43966" N	76° 20' 04.14930" W	3.83	4.02	4.14	104	0
11/13	1:34 pm	Site 007: Queenstown Boat Landing	38° 59' 23.97891" N	76° 09' 39.41303" W	5.23	5.23	5.61	87	1.2, from W
11/13	3:59 pm	Site 007: Queenstown Boat Landing	38° 59' 23.97891" N	76° 09' 39.41303" W	4.68	4.62	4.65	79	0-0.6, from E
11/14	10:12 am	Site 007: Queenstown Boat Landing	38° 59' 23.97891" N	76° 09' 39.41303" W	3.88	3.91	4.08	*90	1.5 to 2.7, from SE
11/19	1:12 pm	Site 008: Green Lane Boat Ramp	39° 07' 50.22312" N	76° 14' 34.21321" W	21.8	21.5	29.2	67	0
11/19	3:11 pm	Site 008: Green Lane Boat Ramp	39° 07' 50.22312" N	76° 14' 34.21321" W	7.30	6.98	7.40	85	0
11/19	1:45 pm	Site 009: Tolchester Marina	39° 12' 54.66214" N	76° 14' 37.90472" W	6.76	5.23	4.27	*7	1.2-3.0, from W
11/19	3:40 pm	Site 009: Tolchester Marina	39° 12' 54.66214" N	76° 14' 37.90472" W	3.32	2.98	3.09	*9	0

Date	Time (UTC - 4)	Location	Latitude	Longitude	Turbidity Read 1 (NTU)	Turbidity Read 2 (NTU)	Turbidity Read 3 (NTU)	Secchi Depth (cm)	Wind Speed (knots)
11/14	12:49 pm	Site 010: Landford Bay Marina	39° 07' 06.27870" N	76° 10' 30.54399" W	9.54	9.80	10.2	56	5.2, from SE
11/18	1:47 pm	Site 010: Landford Bay Marina	39° 07' 06.27870" N	76° 10' 30.54399" W	6.92	7.37	6.96	89	2.0, from WSW
11/18	4:35 pm	Site 010: Landford Bay Marina	39° 07' 06.27870" N	76° 10' 30.54399" W	7.92	8.32	7.59	64	0
11/14	9:20 am	Site 011: Centreville Public Landing	39° 03' 15.46736" N	76° 04' 27.49833" W	10.2	9.10	9.09	61	2.8, from ESE
11/14	11:07 am	Site 011: Centreville Public Landing	39° 03' 15.46736" N	76° 04' 27.49833" W	9.07	9.03	9.12	60	9.8, from E
11/14	2:01 pm	Site 011: Centreville Public Landing	39° 03' 15.46736" N	76° 04' 27.49833" W	7.66	7.80	8.34	59	6 to 7.8, from E
11/18	3:45 pm	Site 012: Bogles Wharf	39° 01' 55.88903" N	76° 12' 34.55081" W	9.73	10.7	10.1	*91	0
11/12	2:49 pm	Site 013: Easton Point Marina	38° 46' 04.58518" N	76° 05' 42.07940" W	12.8	13.1	12.7	51	4.0 to 7.1, from E
11/13	9:03	Site 013: Easton Point Marina	38° 46' 04.58518" N	76° 05' 42.07940" W	11.2	12.1	11.3	59	3 to 5.6, from N
11/16	11:30 am	Site 014: Ferry Point Nature Park	38° 58' 46.39679" N	76° 14' 55.28450" W	11.2	11.2	11.5	*50	4.0 to 5.8, from NE
11/16	1:58 pm	Site 015: Quaker Neck Landing	39° 07' 47.05619" N	76° 05' 48.89269" W	7.06	7.92	8.75	86	1.2 to 2.8, from W
11/17	3:47 pm	Site 016: Cliff City Boat Ramp	39° 06' 24.91069" N	76° 08' 31.99764" W	9.17	10.6	9.53	*116	1.7, from SW

** Measurement is depth to the bottom surface due to observational depth limitations*

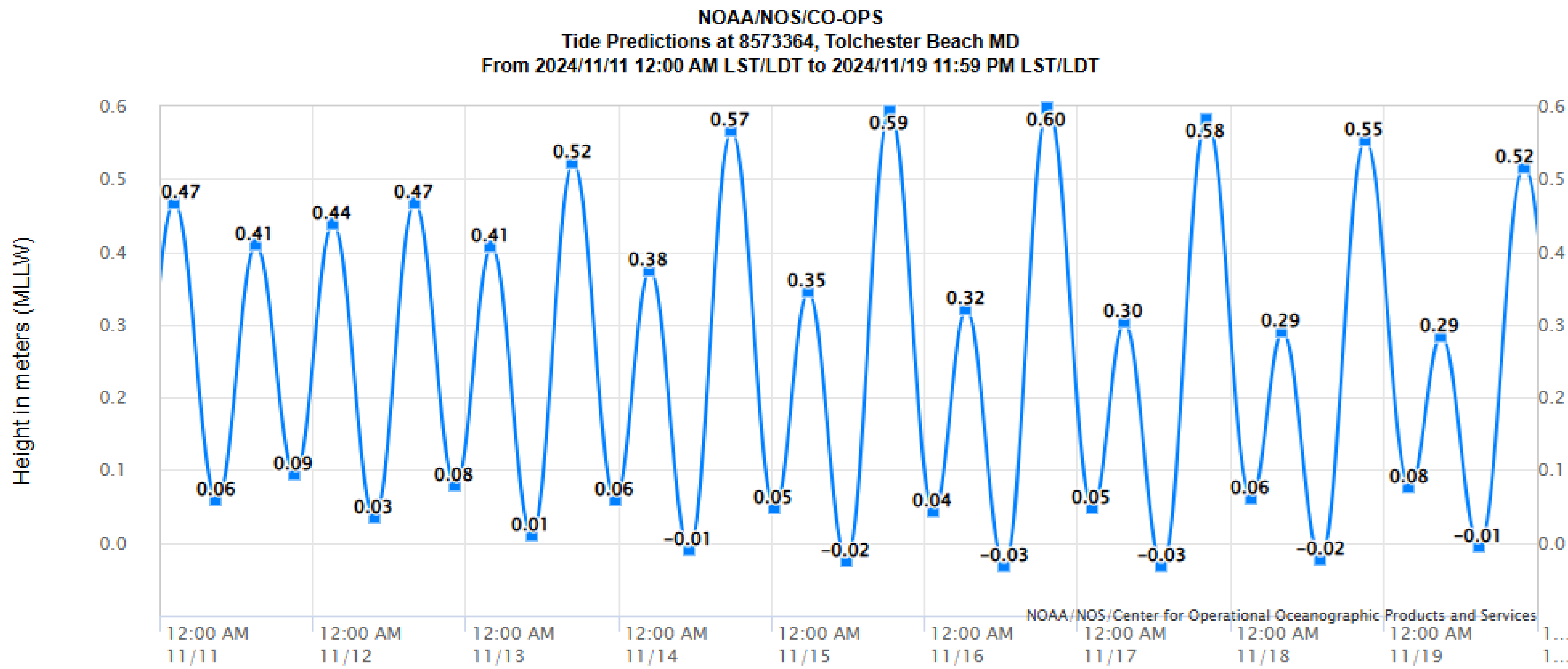

Figure 2: Tide Predictions at 8573364, Tolchester Beach, Maryland during the time of lidar acquisition

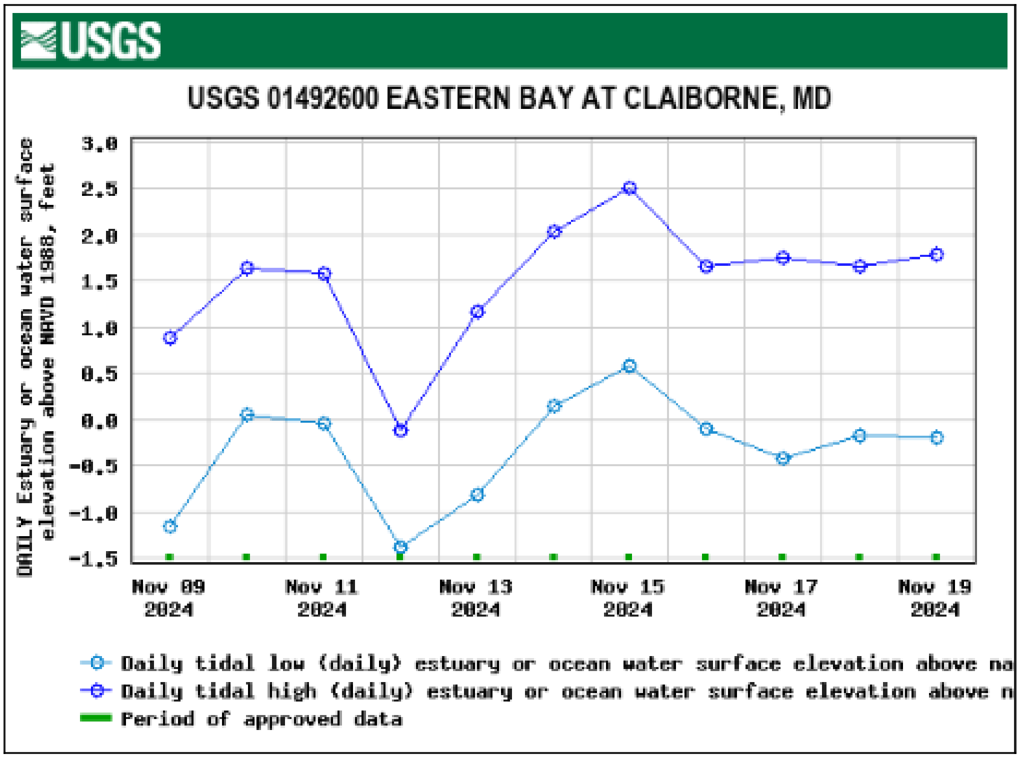

Figure 3: USGS Station 01492600 surface elevation along the Eastern Bay at Claiborne, Maryland at the time of lidar acquisition

Figure 4: These photos taken by NV5 acquisition staff display water clarity conditions at two locations within the NOAA Chesapeake site

Airborne Lidar Survey

The lidar survey was accomplished using a Chiroptera 4X (CH4X) green laser system mounted in a Cessna Grand Caravan, and imagery collected was collected using a Beechcraft Super King Air. The CH4X sensor allows for a depth penetration of K*Dmax=2.7. The CH4X performs well in dynamic wave action and automatically corrects for water refraction, making it useful in collecting shallow coastal and shoreline data. It detects obstructions, such as vegetation and anthropogenic features, with oblique lidar. This means it can provide additional information from multiple positions that more closely resembles the actual features and allows for more analyses than traditional imagery. This system provides seamless integration between the NIR and Green channels as well as between the onshore and shoreline data.

The CH4X laser system was dually mounted with an additional Leica 40kHZ deep bathymetric channel known as a Leica HawkEye 4X (HE4X). Because of its design and a higher density point cloud, the HE4X is able to provide better resolution and depth penetration (up to 50 meters in optimal conditions) than the CH4X shallow green laser at the same wavelength (515 nm). However, it is not designed for shallower areas, which are acquired with the CH4X shallow green sensor. The bathymetric sub-systems of the HE4X use a palmer scanner to produce an elliptical scan pattern of laser points with a degree of incidence ranging from +/-14° (front and back) to +/-20° (sides), providing a 40° field of view. This has the benefit of providing multiple look angles on a single pass and helps to eliminate shadowing effects. This can be of particular use for bathymetric features (e.g., sides of narrow water channels; features on the seafloor such as smaller objects and wrecks). The bathymetric laser is a diode-pumped class 4 laser.

Both the CH4X and HE4X systems acquire full waveform data for every pulse. The recorded waveform enables range measurements for all discernible targets for a given pulse. It is not uncommon for some types of surfaces (e.g., dense vegetation or water) to return fewer pulses to the lidar sensor than the laser originally emitted. The discrepancy between first return and overall delivered density will vary depending on terrain, land cover, and the prevalence of water bodies. All discernible laser returns were processed for the output dataset. Table 5 summarizes the settings used to yield an average pulse density of at least 3 and 4 pulses/m^2 for bathymetric and NIR returns, respectively, over the NOAA Chesapeake project area. Figure 5 shows the flightlines acquired using these lidar specifications.

Table 5: Lidar specifications and aerial survey settings

Parameter	NIR Sensor	Shallow Green Sensor	Deep Green Sensor
Acquisition Dates	11/9/24 – 11/19/24	11/9/24 – 11/19/24	11/9/24 – 11/19/24
Aircraft Used	Cessna Grand Caravan	Cessna Grand Caravan	Cessna Grand Caravan
Sensor	Leica Chiroptera 4X	Leica Chiroptera 4X	Leica HawkEye 4X
Laser Channel	NIR	Green (shallow)	Green (deep)
Resolution/Density	Average 4 points/m²	Average 3 points/m²	Average 3 points/m²
Nominal Pulse Spacing	0.5 m	0.58 m	0.58 m
Survey Altitude (AGL)	400 m	400 m	400 m
Survey speed	145 knots	145 knots	145 m
Field of View	40°	40°	40°
Mirror Scan Rate	4200 RPM	3500 RPM	1880 RPM
Target Pulse Rate	250 kHz	50 kHz	10 kHz
Pulse Length	2.5 ns	2.5 ns	2.5 ns
Laser Pulse Footprint Diameter	10 cm	160 cm	288 cm
Central Wavelength	1064 nm	515 nm	515 nm
Pulse Mode	Continuous Multipulse	Continuous Multipulse	Continuous Multipulse
Beam Divergence	0.25 mrad	4.0 mrad	7.2 mrad
Swath Width	291 m	291 m	291 m
Swath Overlap	25%	25%	25%
Intensity	16-bit	16-bit	16-bit
Horizontal Accuracy	1 m	1 m	1 m

All areas were surveyed with an opposing flightline side-lap of at least 25% (at least 50% overlap) in order to reduce laser shadowing and increase surface laser painting. To accurately solve for laser point position (geographic coordinates x, y, and z), the positional coordinates of the airborne sensor and the orientation of the aircraft to the horizon (attitude) were recorded continuously throughout the lidar data collection mission. Position of the aircraft was measured twice per second (2 Hz) by an onboard differential GPS unit, and aircraft attitude was measured 200 times per second (200 Hz) as pitch, roll, and yaw (heading) from an onboard inertial measurement unit (IMU). To allow for post-processing correction and calibration, aircraft and sensor position and attitude data are indexed by GPS time.

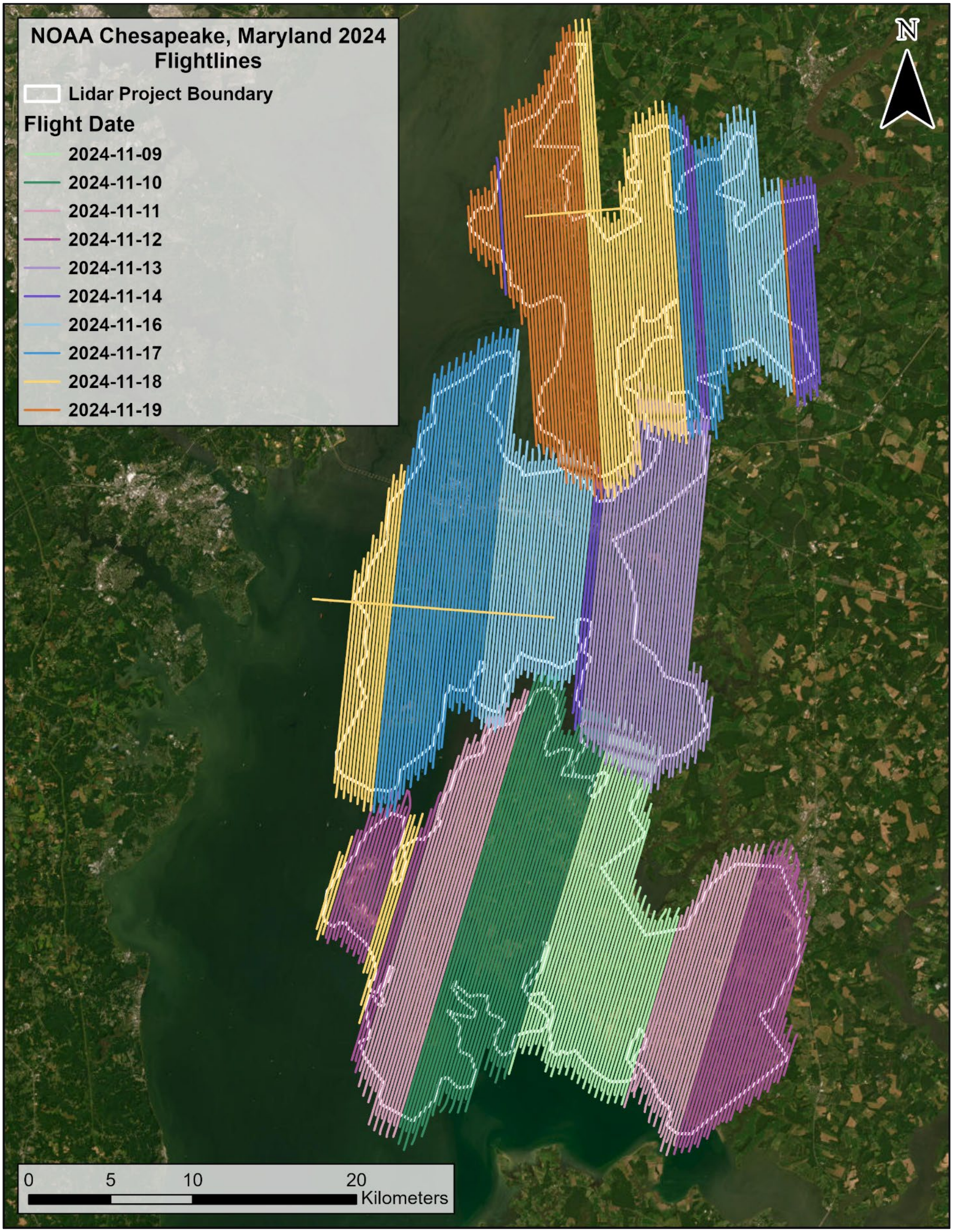

Figure 5: Flightlines map

Ground Survey

Ground control surveys, including monumentation, aerial targets, and ground survey points (GSPs), were conducted to support the airborne acquisition. Ground control data were used to geospatially correct the aircraft positional coordinate data and to perform quality assurance checks on final lidar data and orthoimagery products.

Base Stations

Base stations were used for collection of GSPs using real time kinematic (RTK) and fast static (FS) survey techniques.

Base station locations were selected with consideration for satellite visibility, field crew safety, and optimal location for GSP coverage. NV5 utilized 5 permanent real-time network (RTN) base stations from the Hexagon SmartNet network for the NOAA Chesapeake lidar project (Table 6, Figure 7). NV5's professional land surveyor, Mark Meade (MDPLS#5256592), oversaw and certified the ground survey. No physical monuments were utilized for this project.

Table 6: Base station positions for the NOAA Chesapeake acquisition. Coordinates are on the NAD83 (2011) datum, epoch 2010.00

Monument ID	Latitude	Longitude	Ellipsoid (meters)	Owner
LOYF	38° 58' 28.07436" N	76° 31' 19.88502" W	-14.529	SmartNet
MDCT	39° 13' 45.21495" N	76° 02' 58.52399" W	-19.011	SmartNet
MDDU	39° 16' 13.13187" N	76° 30' 07.54624" W	-14.077	SmartNet
MDNM	38° 33' 29.58759" N	75° 59' 12.76582" W	-21.055	SmartNet
MDUM	38° 49' 00.68897" N	76° 45' 06.93394" W	-12.564	SmartNet

NV5 utilized static Global Navigation Satellite System (GNSS) data collected at 1 Hz recording frequency for each base station. During post-processing, the static GNSS data was triangulated with nearby Continuously Operating Reference Stations (CORS) using the Online Positioning User Service (OPUS[1]) for precise positioning. Multiple independent sessions over the same monument were processed to confirm antenna height measurements and to refine position accuracy.

[1] OPUS is a free service provided by the National Geodetic Survey to process corrected monument positions: OPUS website

Ground Survey Points

GSPs were collected using RTK and FS survey techniques. For RTK surveys, a roving receiver receives corrections from a nearby base station or RTN via radio or cellular network, enabling rapid collection of points with relative errors less than 1.5 cm horizontal and 2.0 cm vertical. FS surveys compute these corrections during post-processing to achieve comparable accuracy. RTK surveys record data while stationary for at least five seconds, calculating the position using at least three one-second epochs. FS surveys record observations for up to fifteen minutes on each GSP in order to support longer baselines. All GSP measurements were made during periods with a Position Dilution of Precision (PDOP) of ≤ 3.0 with at least six satellites in view of the stationary and roving receivers. See Table 7 for NV5 ground survey equipment information.

Forested checkpoints are collected using total stations to measure positions under dense canopy. Total station backsight and setup points are established using GNSS survey techniques.

GSPs were collected in areas where good satellite visibility was achieved on paved roads and other hard surfaces such as gravel or packed dirt roads. GSP measurements were not taken on highly reflective surfaces such as center line stripes or lane markings on roads due to the increased noise seen in the laser returns over these surfaces. GSPs were collected within as many flightlines as possible; however, the distribution of GSPs depended on ground access constraints and monument locations and may not be equally distributed throughout the study area (Figure 7).

Table 7: NV5 ground survey equipment identification

Receiver Model	Antenna	OPUS Antenna ID	Use
Trimble R12	Integrated Antenna	TRMR12	Rover

Aerial Targets

Air target points (ATPs) were collected throughout the project area prior to imagery acquisition to refine the exterior orientation parameters of the camera and conduct an accuracy assessment of the final orthophoto product (Figure 7). ATPs are typically collected over hard surface ground features or temporary vinyl chevrons. Hard surface points consist of high contrast, road markings such as stop bars and turn arrows and cement corners. Each ATP was surveyed using FS or RTK techniques.

Figure 6: Examples of aerial targets

Land Cover Class

In addition to ground survey points, land cover class checkpoints were collected throughout the study area to evaluate vertical accuracy. Vertical accuracy statistics were calculated for all land cover types to assess confidence in the lidar derived ground models across land cover classes (Table 8, see Lidar Accuracy Assessments, page 35).

Table 8: Land cover types and descriptions

Land cover type	Land cover code	Example	Description	Accuracy Assessment Type
Shrub	SH		Low growth shrub	VVA
Tall Grass	TG		Herbaceous grasslands in advanced stages of growth	VVA
Forest	FR		Forested areas	VVA
Bare Earth	BE		Areas of bare earth surface	NVA
Urban	UA		Areas dominated by urban development, including parks	NVA

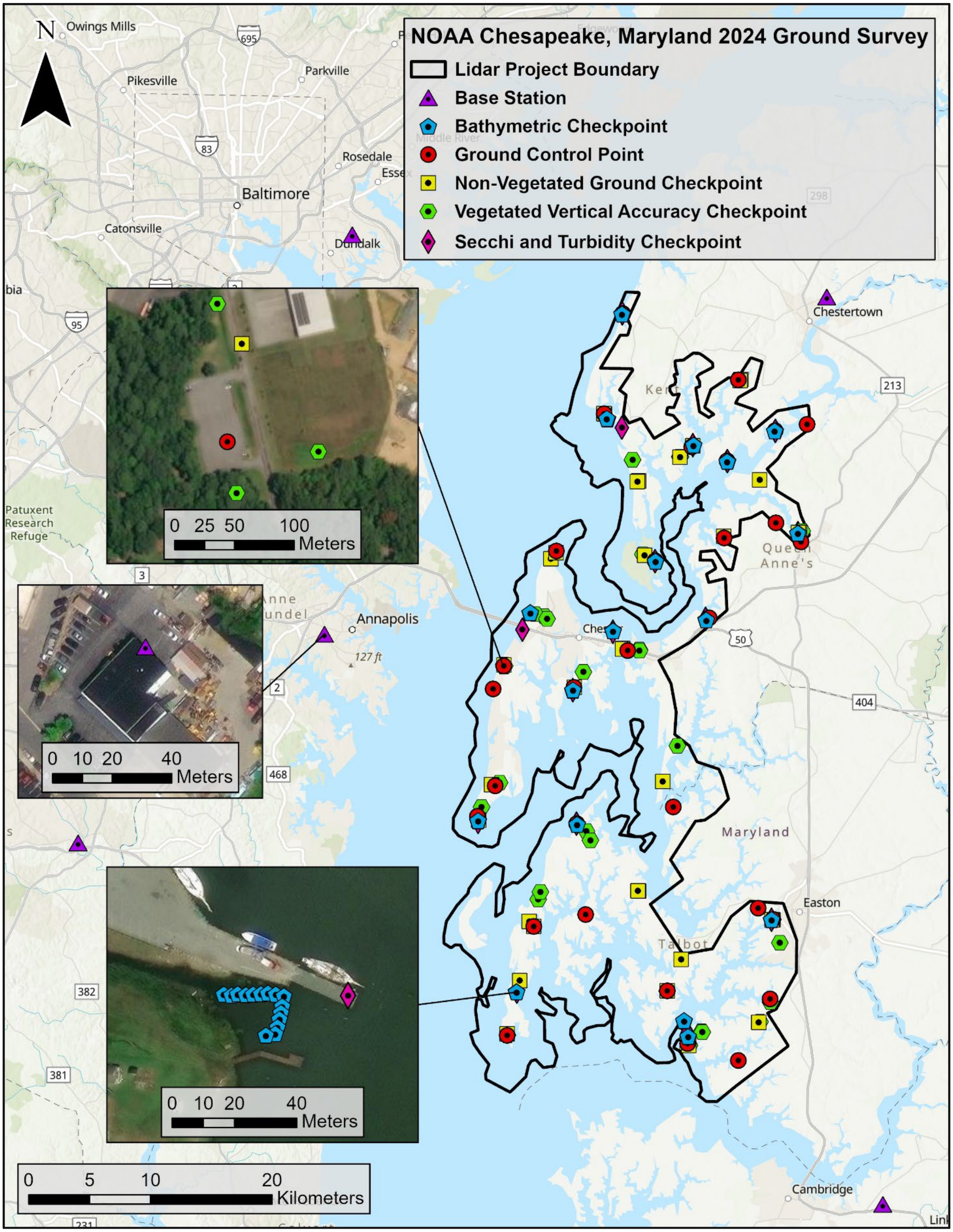

Figure 7: Ground survey location map

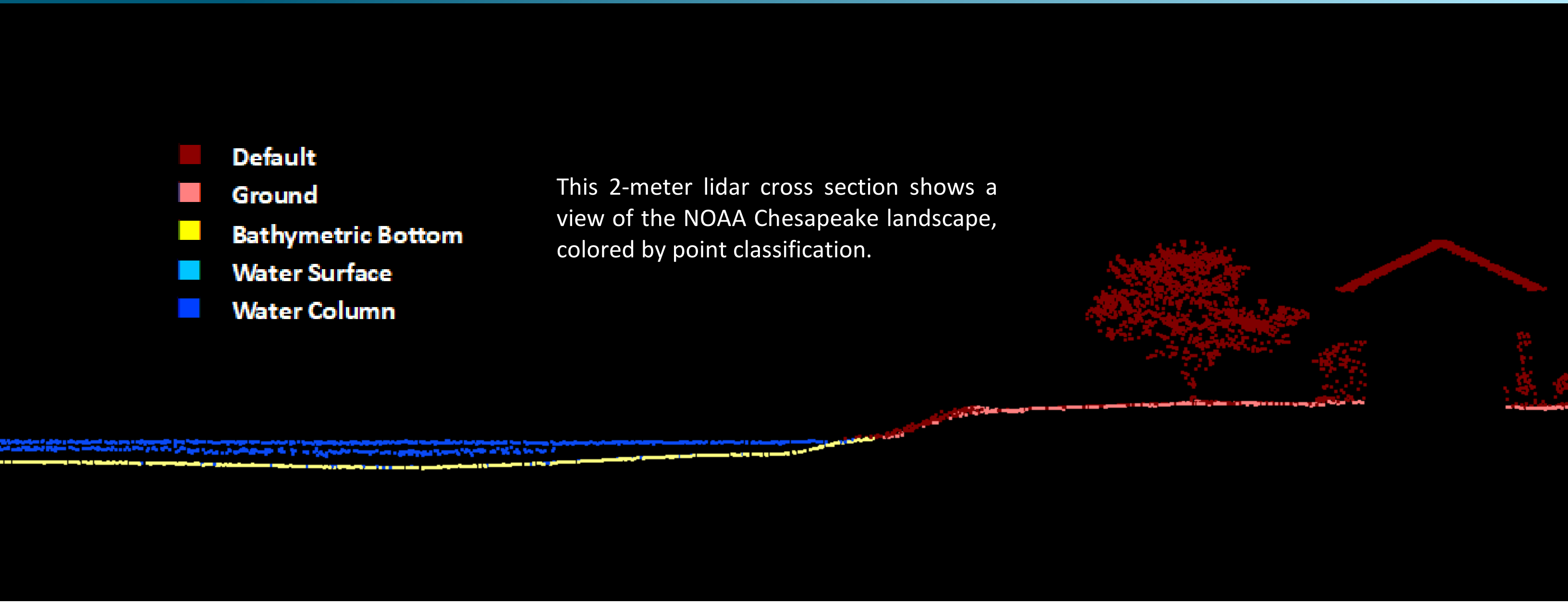

This 2-meter lidar cross section shows a view of the NOAA Chesapeake landscape, colored by point classification.

Boresight Calibration

Prior to the lidar acquisition, NV5 collects sample lidar data in support of sensor calibration and geometric adjustments for all sensor and aircraft combinations utilized in the airborne acquisition. These data support boresight analysis to properly position the sensor orientation within the aircraft. This process is essential for data interswath adjustments performed during the calibration phase. Additional details on geometric adjustments can be found in Appendix A - Accuracy Controls.

Topobathymetric Lidar Data

Upon completion of data acquisition, NV5 processing staff initiated a suite of automated and manual techniques to process the data into the requested deliverables. Processing tasks included GPS control computations, smoothed best estimate trajectory (SBET) calculations, kinematic corrections, calculation of laser point position, sensor and data calibration for optimal relative and absolute accuracy, and lidar point classification. The point classification scheme used is detailed in Table 9, brief descriptions of processing tasks are shown in Table 10, and example raster layers for processing and review can be visualized in Figure 8. Processing methodologies were tailored to the NOAA Chesapeake landscape.

Table 9: ASPRS LAS classification standards applied to the NOAA Chesapeake dataset

Classification Number	Classification Name	Classification Description
1	Unclassified	Processed, but unclassified
2	Ground	Bare earth ground
7-Withheld	Low Noise	Noise (low manually identified)
18-Withheld	High Noise	Noise (high manually identified)
20	Ignored Ground	Ground point in breakline proximity
21	Snow	Identifiable snow
22	Temporal Exclusion	Denotes Unclassified and Ground associated temporal changes from varying lifts, not utilized in the topographic point class
40	Bathymetric Bottom	Bathymetric point (e.g., seafloor or riverbed; also known as submerged topography)
41	Water Surface	Water's surface (sea/river/lake surface) from topographic-bathymetric lidar
42-Synthetic	Derived Water Surface	Synthetic water surface location used in computing refraction at water surface
43	Submerged Feature	Submerged object, not otherwise specified (e.g., wreck, rock, submerged piling)
44	S-57 Object	International Hydrographic Organization (IHO) S-57 object, not otherwise specified
45	Water Column	Refracted returns not determined to be water surface or bathymetric bottom
46	Submerged Aquatic Vegetation	Benthic vegetation in submerged, refracted areas
47-Withheld	Bathymetric Noise	Bathymetric noise below water surface
48	Submerged Temporal Exclusion	Denotes Bathymetric Bottom and Water Column temporal changes from varying lifts, not utilized in the bathymetric point class
1-Withheld	Edge Clip	Unclassified points flagged as withheld. These are primarily "edge" points from the higher scan angle being removed
1-Overlap Withheld	Unrefracted Green Chiroptera Points	Unrefracted green data from the Chiroptera 4X system

Original SOW classification scheme	Delivered in LAS files
Additional classification codes	Delivered in LAS files
Original SOW classification code not used	Not delivered in LAS files
Deleted points	Not delivered in LAS files

Table 10: Lidar processing workflow

Lidar Processing Step	Software Used
Resolve kinematic corrections for aircraft position data using kinematic aircraft GPS and static ground GPS data. Develop a SBET file that blends post-processed aircraft position with sensor head position and attitude recorded throughout the survey.	Inertial Explorer v.9.00
Calculate laser point position by associating SBET position to each laser point return time, scan angle, intensity, etc. Create raw laser point cloud data for the entire survey in *.las (ASPRS v. 1.4) format. Convert data to orthometric elevations by applying a geoid correction.	Lidar Survey Studio v.3.4.3 Las Projector 1.6 (NV5 proprietary software)
Import raw laser points into manageable blocks to perform manual relative accuracy calibration and filter erroneous points. Classify ground points for individual flightlines.	TerraScan v.19.005
Using ground classified points per flightline, test the relative accuracy. Perform automated line-to-line calibrations for system attitude parameters (pitch, roll, heading), mirror flex (scale) and GPS/IMU drift. Calculate calibrations on ground classified points from paired flightlines and apply results to all points in a flightline. Use every flightline for relative accuracy calibration.	StripAlign v.2.25
Apply refraction correction to all subsurface returns.	Lidar Survey Studio v.3.4.3 Las Monkey v.2.6.9 (NV5 proprietary software)
Classify resulting data to ground and other client designated ASPRS classifications (Table 9). Assess statistical absolute accuracy via direct comparisons of ground classified points to ground control survey data.	TerraScan v.19.005 TerraModeler v.19.003
Generate bare earth models as triangulated surfaces. Generate highest hit models as a surface expression of all classified points. Export all surface models as Cloud-Optimized GeoTIFFs at a 1-meter pixel resolution.	TerraScan v.19.005 TerraModeler v.19.003 Las Product Creator v.4.0 (NV5 proprietary software) ArcMap v.10.3 and 10.8
Correct intensity values for variability and export intensity images as Cloud-Optimized GeoTIFFs at a 1-meter pixel resolution.	Las Monkey v.2.6.9 (NV5 proprietary) TerraScan v.19.005 TerraModeler v.19.003 ArcMap v.10.3 and 10.8 Las Product Creator v.4.0 (NV5 proprietary software)

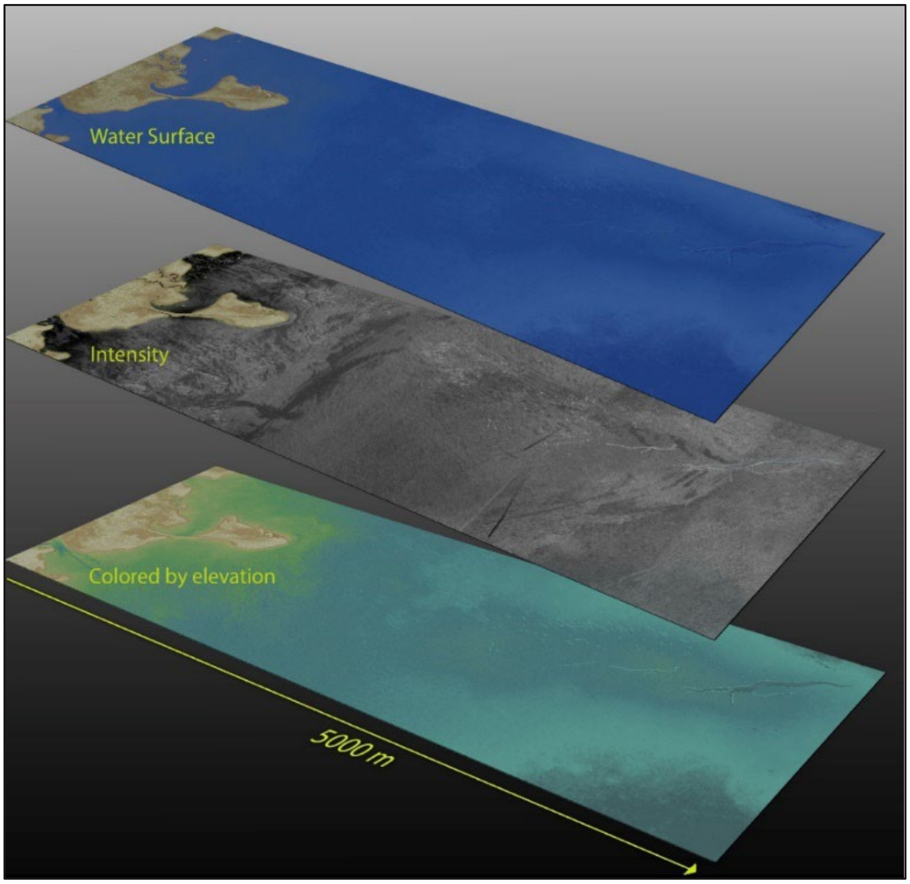

Figure 8: Example processing data layers

GNSS-Inertial Processing

Inertial Explorer software was used for post-processing of airborne GPS and inertial data (IMU), which is critical to the positioning and orientation of the lidar sensor during all flights. The post-processing combines aircraft raw trajectory data with stationary GNSS base station data yielding an SBET necessary for additional post processing software to develop the resulting geo-referenced point cloud from the lidar missions.

During the sensor trajectory processing (combining GNSS & IMU datasets) certain statistical graphs and tables are generated within the software processing environment which are commonly used as indicators of processing stability and accuracy. This data for analysis includes max horizontal and vertical GPS variance, separation plot, altitude plot, PDOP plot, base station baseline length, processing mode, number of satellite vehicles, and mission trajectory.

Bathymetric Refraction

Green lidar pulses that map bathymetry must have their position corrected for the refraction of the light as it enters the water, which results in a change in speed and direction described by Snell's Law. This correction was applied as part of the raw data extraction process in Leica's Lidar Survey Studio (LSS) software. To determine how much time the laser pulse spent traveling through water and at what angle it entered, water surface models (WSMs) were developed for each flightline swath to cover all submerged returns. Synthetic points representing the water surface were generated automatically based on information derived primarily from the sensor’s NIR channel; the NIR wavelength of light does not penetrate the water and therefore generally provides the most consistent information about the surface. The NIR and green channels are coaligned, meaning water surfaces based on NIR are representative of the associated green pulses and can help accurately model even variable water surfaces with tide changes or wave action. The use of synthetic points makes it clear in the point cloud exactly where the water surfaces were placed, especially over any localized areas where the algorithm interpolated or extrapolated the surface to ensure complete coverage of submerged points.

Once the WSMs were generated, LSS applied a refraction correction to each submerged point by intersecting the trajectory of the green pulses with their WSM to determine the angle of incidence with the water surface and the submerged component of the pulse vector. This provides the information necessary to correct the position of underwater points by adjusting the submerged vector length and orientation. After the refraction correction was applied, the point cloud was reviewed for any improper placement of water surface, and any areas identified were reprocessed with adjusted parameters to ensure accurate positioning and classification. Finally, the submerged points were compared against bathymetric checkpoints to assess absolute accuracy.

Lidar Derived Products

Because hydrographic laser scanners penetrate the water surface to map submerged topography, this affects how the data should be processed and presented in derived products from the lidar point cloud. The following section discusses certain derived products that vary from the traditional (NIR) specification and delivery format.

Topobathymetric Digital Elevation Models

Bathymetric bottom returns can be limited by depth, water clarity, and bottom surface reflectivity. Water clarity and turbidity affect the depth penetration capability of the green wavelength laser with returning laser energy diminishing by scattering throughout the water column. Additionally, the bottom surface must be reflective enough to return remaining laser energy back to the sensor at a detectable level. Although the predicted depth penetration range of the CH4X sensor is 1.5 times and the HE4X is 3 times the recorded Secchi depth on brightly reflective surfaces, it is not unexpected to have no bathymetric bottom returns in turbid or non-reflective areas. Since the HE4X is designed specifically for deeper waters, it is expected to have fewer returns in shallower waters.

As a result, creating DEMs presents a challenge with respect to interpolation of areas with no returns. Traditional DEMs are “unclipped”, meaning areas lacking ground returns are interpolated from neighboring ground returns (or breaklines in the case of hydro-flattening), with the assumption that the interpolation is close to reality. In bathymetric modeling, these assumptions are prone to error because a lack of bathymetric returns can indicate a change in elevation that the laser can no longer map due to increased depths. The resulting void areas may suggest greater depths, rather than similar elevations from neighboring bathymetric bottom returns. Therefore, NV5 created a water polygon with bathymetric coverage to delineate areas with successfully mapped bathymetry. This shapefile was used to control the extent of the delivered clipped topobathymetric model to avoid false triangulation (interpolation from TIN’ing) across areas in the water without bathymetric bottom returns.

Normalized Bathymetric Bottom Reflectance

A lidar echo return signal has a recorded amplitude associated for each point and is logged in LAS files as an Intensity record. Laser return intensity is generally a unitless measure of discrete return signal strength, stored as a 16-bit integer value (0 to 65,535). Intensity values roughly correspond to the reflectivity of the surface, which is a function of surface material composition. The magnitude of intensity values can vary across similar surfaces due to variability in atmospherics, water clarity, range, submerged depth, and the angle of incidence on the object. The result is line to line inconsistency and streaking in the images that can reduce the utility of these data for analytics. The Intensity value in the LAS file has been updated with corrected values that have normalized the effects of the variables described above.

When a laser pulse enters the water column, the return signal fades exponentially with depth (Figure 9 and Figure 10); the diminishing rate depends on water properties such as turbidity and composition. This exponential decay can be corrected after determining the rate of decline by comparing similar substrates across multiple flightlines and varying depths. The seabed intensity values for this dataset have been normalized for depth, angle of incidence, and absolute flying altitude (Figure 11). Please note that intensity values are still subject to localized changes of water properties within the water column across a water body.

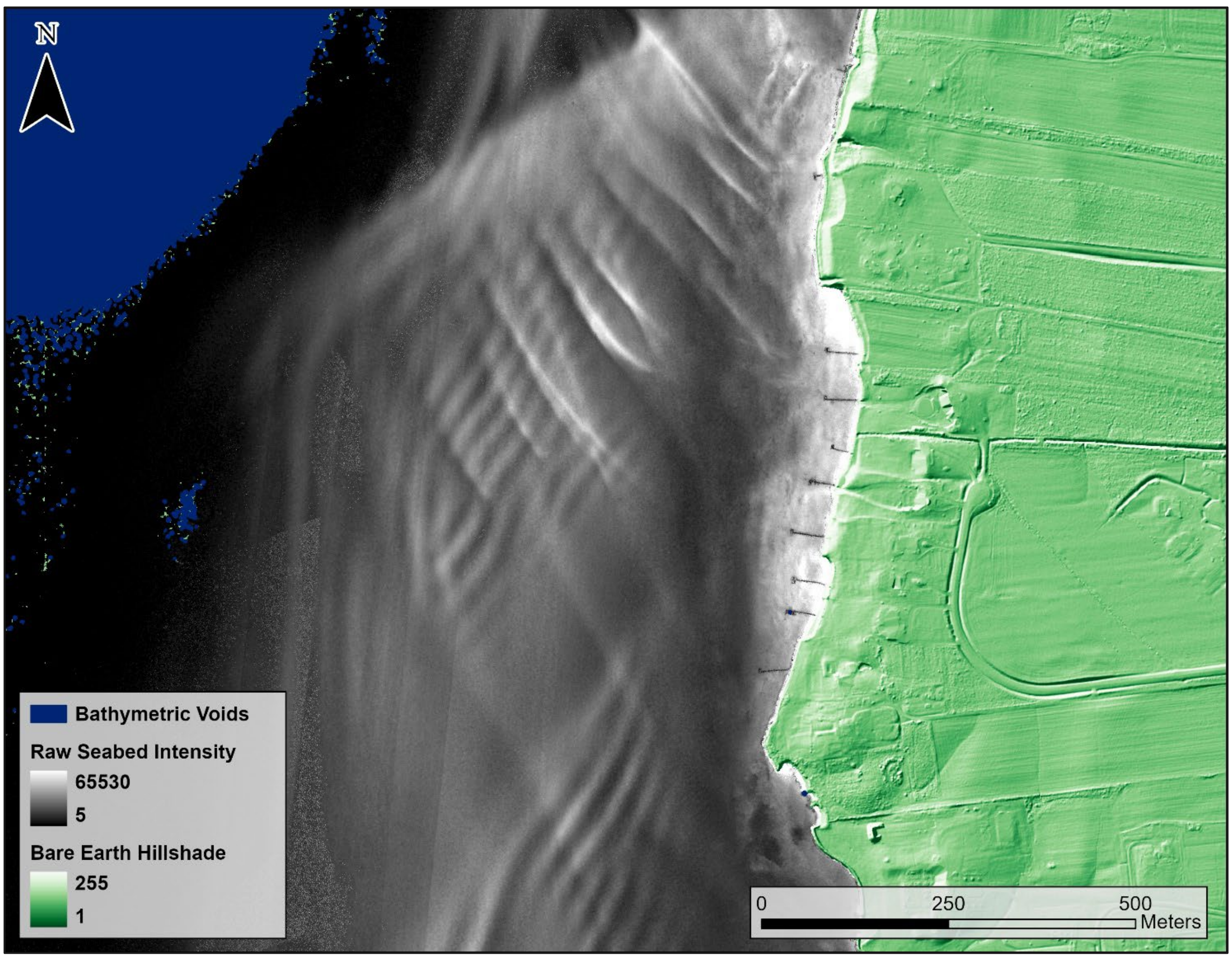

Figure 9: View of raw bathymetric bottom intensity values in the Chesapeake project area

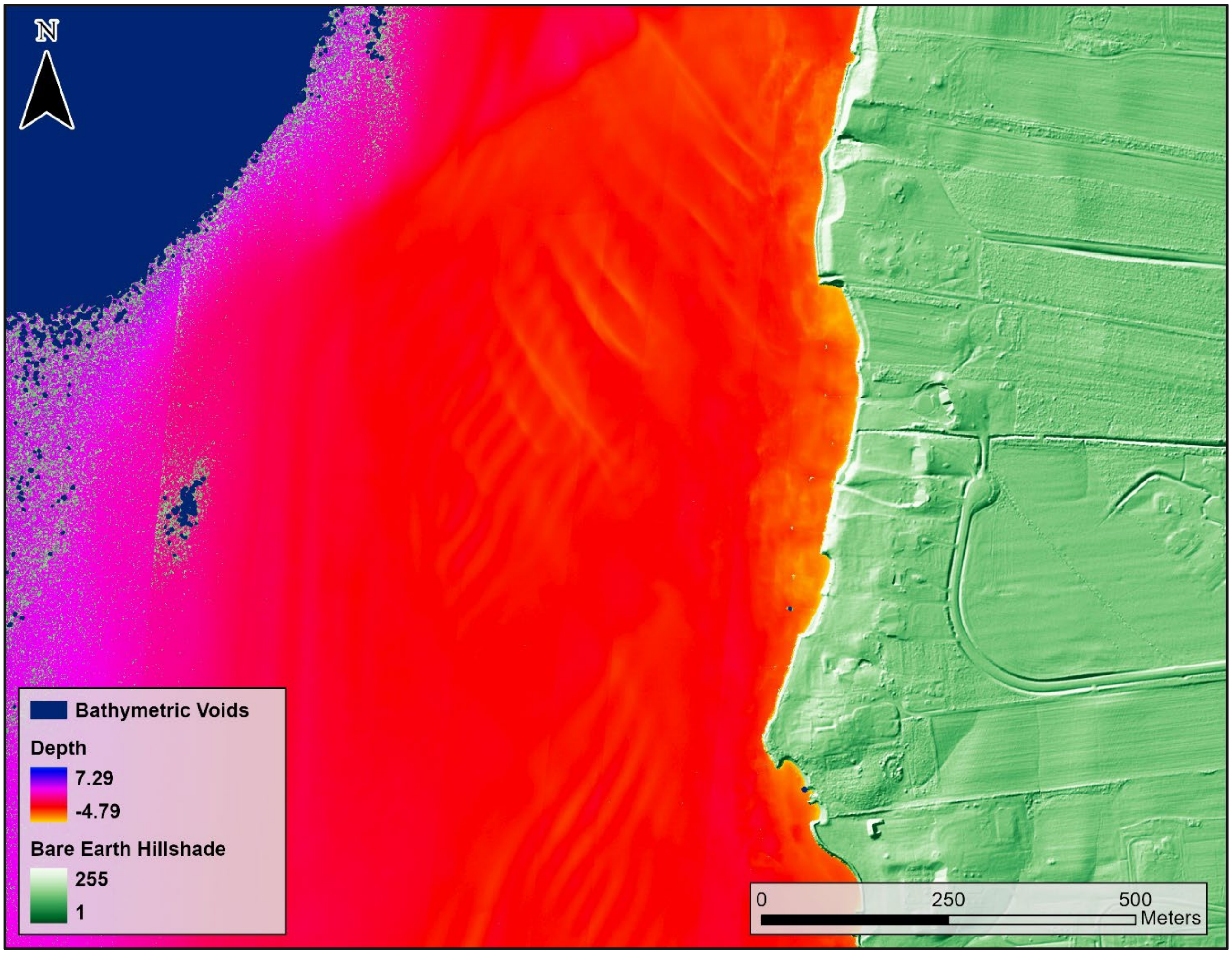

Figure 10: View of the depth raster shows areas of deeper bathymetry which correlated to diminished bathymetric bottom intensity values in the Chesapeake project area.

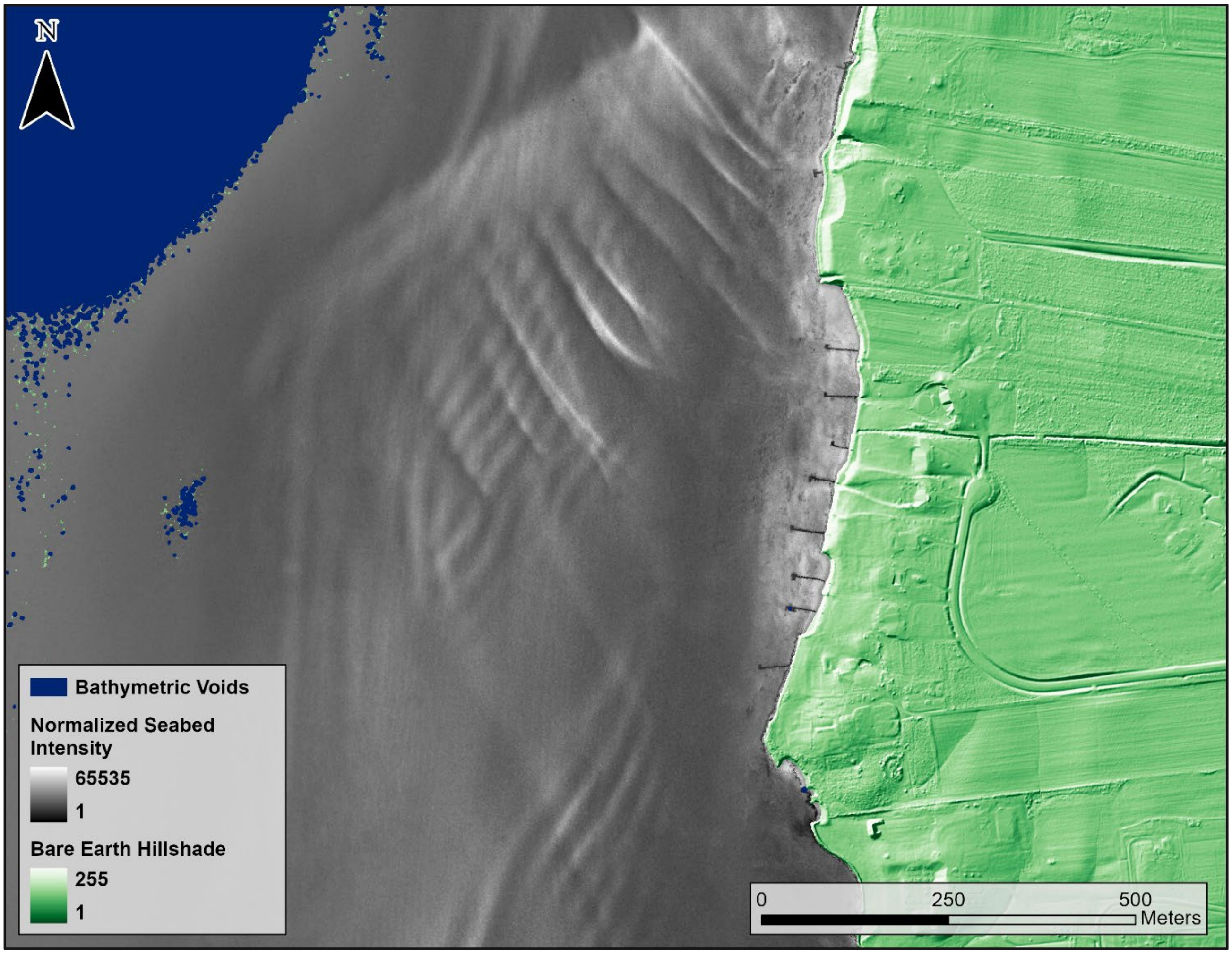

Figure 11: A view of bathymetric bottom Intensity values that were normalized for depth, angle of incidence, and absolute flying altitude in the Chesapeake project area.

Total Propagated Uncertainty

In conjunction with NOAA NGS's effort to maintain and update nautical charts, NV5 supports the need for mapping total propagated uncertainty (TPU) of the NOAA Chesapeake lidar data. TPU values are dependent on both horizontal and vertical uncertainty calculations for bathymetric bottom lidar returns. NOAA's cBlue software was used for calculating the uncertainty estimates.[2] The cBlue tool computes subaerial components of the laser pulse's travel path utilizing information from associated SBETs and lidar sensor model. cBLUE calculates the subaqueous components of a bathymetric laser pulse with Monte Carlo ray tracing simulations that consider environmental factors at the time of lidar acquisition such as wind speed, water clarity, and depth. The resulting subaerial and subaqueous estimates of uncertainty are combined to produce total propagated horizontal and vertical uncertainty values at 95% confidence.

cBLUE outputs javascript object notation (json) metadata files and LAS files appended with TPU data stored in extra bytes. NV5 created 2-band raster models with 1 square meter resolution using bathymetric bottom or submerged object classified points. Band 1 holds the total horizontal uncertainty (THU) 95% confidence values; Band 2 holds the total vertical uncertainty (TVU) 95% confidence values.

[2] NOAA cBlue: https://noaa-rsd.github.io/cBLUE.github.io/index.html

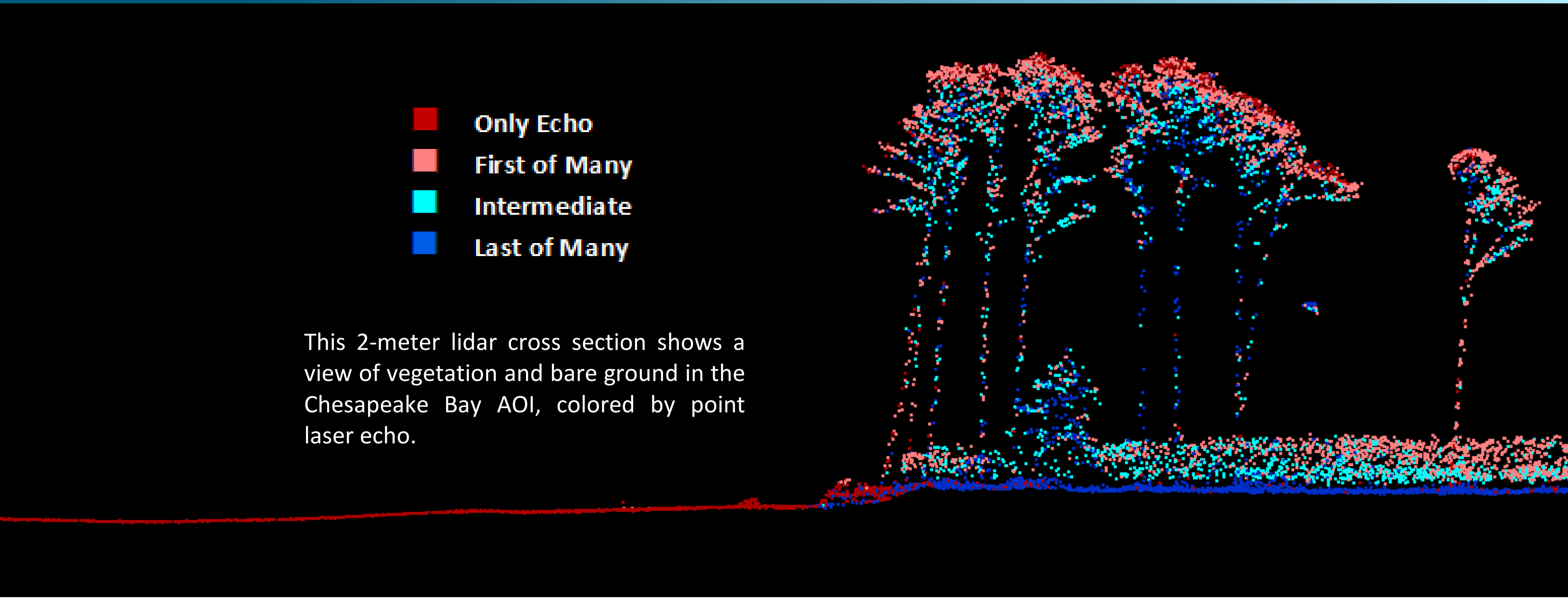

This 2-meter lidar cross section shows a view of vegetation and bare ground in the Chesapeake Bay AOI, colored by point laser echo.

Bathymetric Lidar

An underlying principle for collecting hydrographic lidar data is to survey near-shore areas that can be difficult to collect with other methods, such as multi-beam sonar, particularly over large areas. The capability and effectiveness of the bathymetric lidar is impacted by several parameters including depth penetrations below the water surface, bathymetric return density, and spatial accuracy.

Mapped Bathymetry and Depth Penetration

Under optimal conditions, the specified depth penetration range of the CH4X is about 1.5 times and the HE4X is 3 times the recorded Secchi depth. Since the HE4X is designed specifically for deeper waters, there were fewer returns from this sensor in shallower areas, which were acquired using the CH4X shallow green sensor. To assist in evaluating performance results of the sensor, a polygon layer was created to delineate areas where bathymetry was successfully mapped.

This shapefile was used to control the extent of the delivered clipped topobathymetric model and to avoid false triangulation across areas in the water with no returns. Insufficiently mapped areas were identified by triangulating bathymetric bottom points with an edge length maximum of 4.56 meters. This ensured all areas of no returns (> 9 m^2) were identified as data voids.

Lidar Point Density

First Return Point Density

The acquisition parameters were designed to acquire an average first-return density of 4 points/m^2 in terrestrial areas and 3 points/m^2 for bathymetric areas. First return density describes the density of pulses emitted from the laser that return at least one echo to the system. Multiple returns from a single pulse were not considered in first return density analysis. Some types of surfaces (e.g., breaks in terrain, water, and steep slopes) may have returned fewer pulses than originally emitted by the laser.

First returns typically reflect off the highest feature on the landscape within the footprint of the pulse. In forested or urban areas, the highest feature could be a tree, building, or power line, while in areas of unobstructed ground, the first return will be the only echo and represents the bare earth surface.

The average first-return density of the NOAA Chesapeake lidar project was 6.83 points/m^2 for the NIR sensor, 4.32 points/m^2 for the green sensors, and 11.15 points/m^2 for the sensors combined (Table 11). First return density for green channel pulses is reduced over deep, calm water due to limited bottom detection and lower water surface reflectivity, resulting in fewer detected returns than pulses emitted. All areas within the AOI, including zones of full extinction, were included in the density reporting, which contributed to a lower overall average. The statistical and spatial distributions of all first return densities per 100 m x 100 m cell are portrayed in Figure 12 to Figure 14 and Figure 16.

Bathymetric and Ground Classified Point Densities

The density of ground classified lidar returns and bathymetric bottom returns were also analyzed for this project. Terrain character, land cover, and ground surface reflectivity all influenced the density of ground surface returns. In vegetated areas, fewer pulses may have penetrated the canopy, resulting in lower ground density. Similarly, the density of bathymetric bottom returns was influenced by turbidity, depth, and bottom surface reflectivity. In turbid areas, fewer pulses may have penetrated the water surface, resulting in lower bathymetric density.

The ground and bathymetric bottom classified density of lidar data for the NOAA Chesapeake project was 5.62 points/m^2 (Table 11). The statistical and spatial distributions per 100 m x 100 m cell of the ground and bathymetric bottom classified return densities are portrayed in Figure 15 and Figure 17.

Additionally, for the NOAA Chesapeake project, density values of only bathymetric bottom returns were calculated for areas containing at least one bathymetric bottom return. Areas lacking bathymetric returns (voids) were not considered in calculating an average density value. Within the successfully mapped area, a bathymetric bottom return density of 5.15 points/m^2 was achieved.

Table 11: Average lidar point densities

Density Type	Point Density
NIR First Returns	6.83 points/m²
Green First Returns	4.32 points/m²
Combined First Returns	11.15 points/m²
Ground and Bathymetric Bottom Classified Returns	5.62 points/m²
Bathymetric Bottom Classified Returns	5.15 points/m²

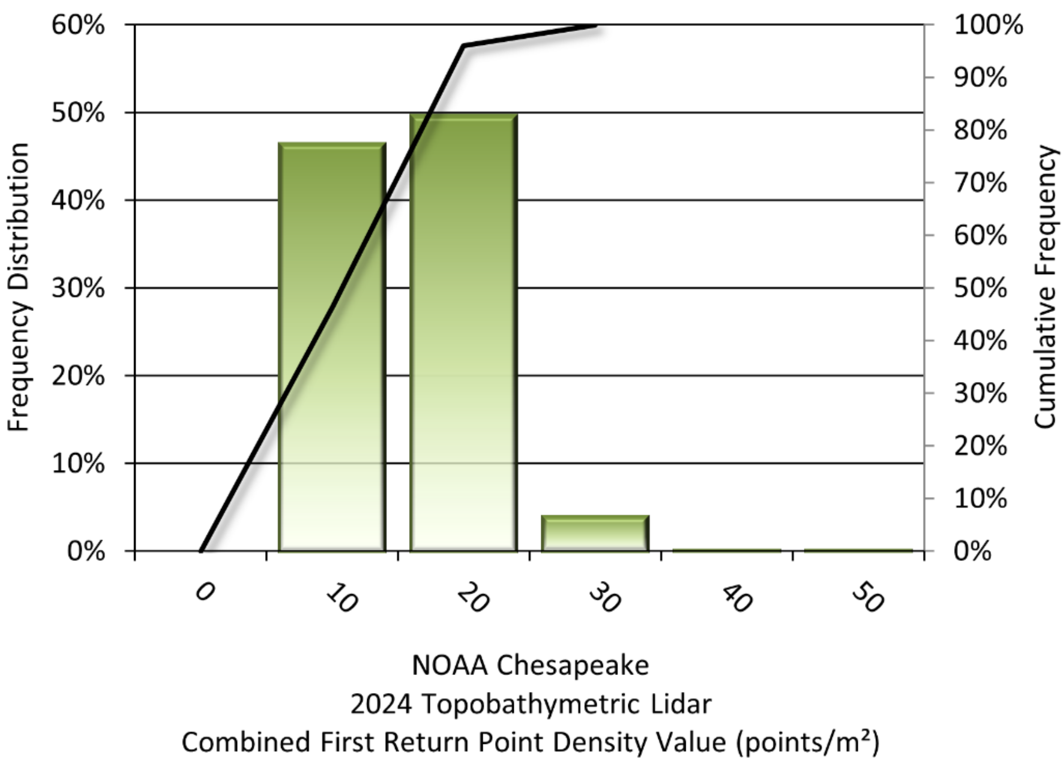

Figure 12: Frequency distribution of first return densities per 100 x 100 m cell for all the sensors

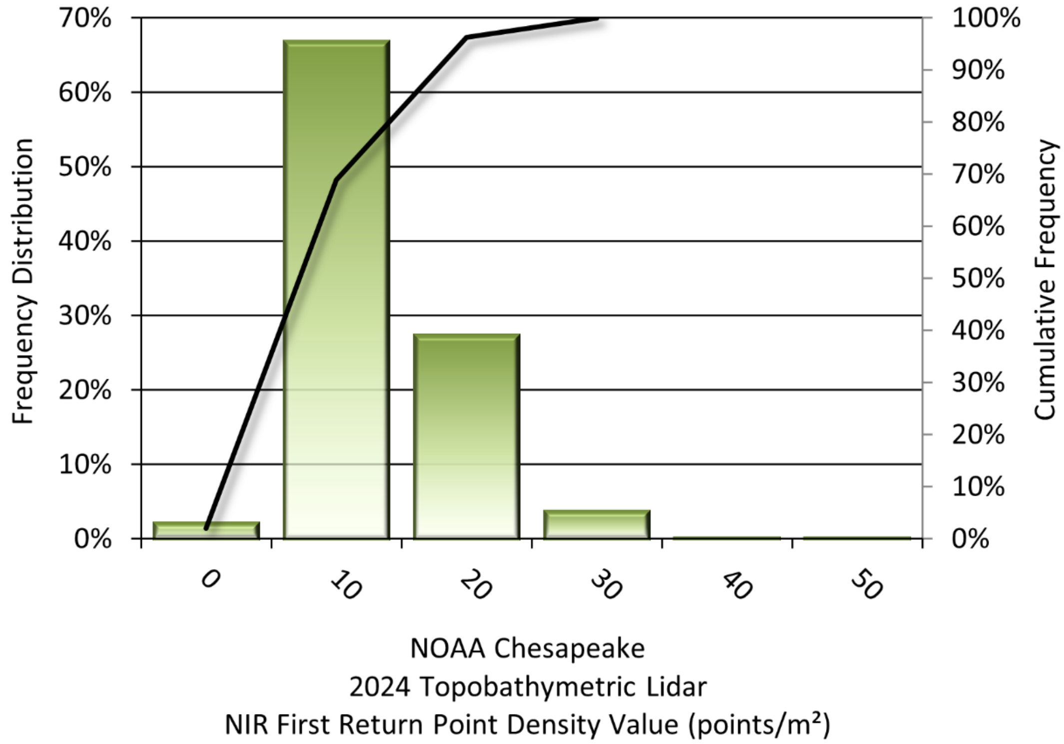

Figure 13: Frequency distribution of first return densities per 100 x 100 m cell for the NIR sensor

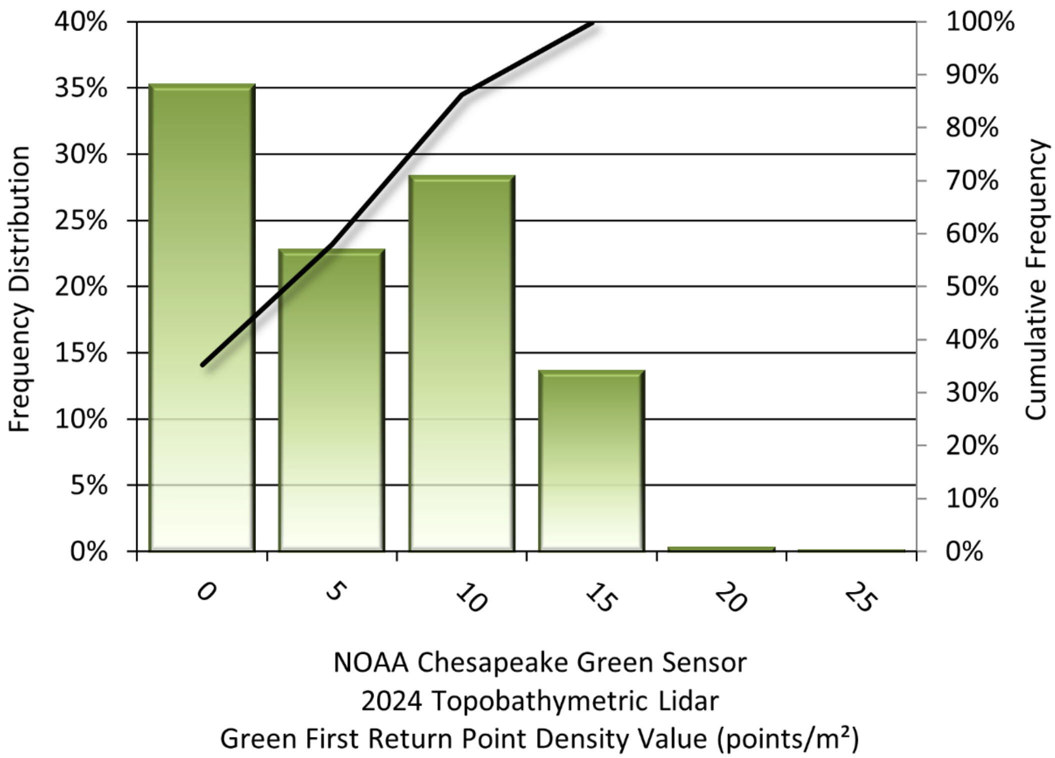

Figure 14: Frequency distribution of first return densities per 100 x 100 m cell for the green sensors

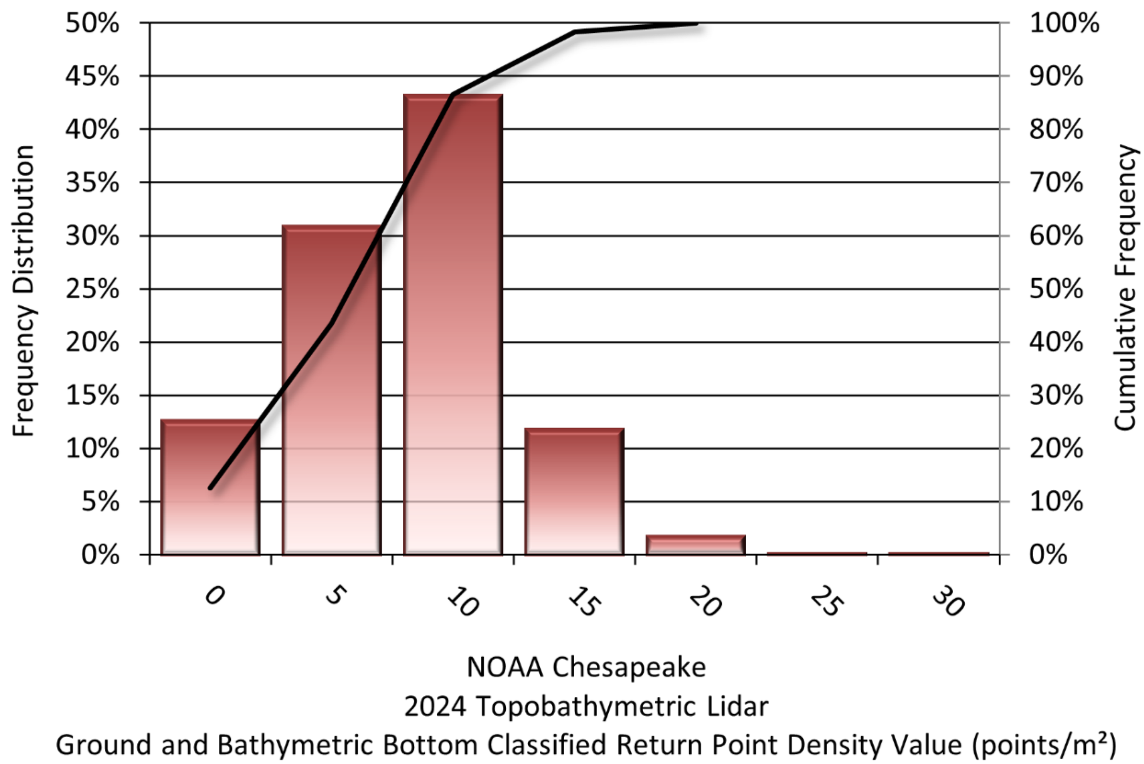

Figure 15: Frequency distribution of ground and bathymetric bottom classified return densities per 100 x 100 m cell for all sensors

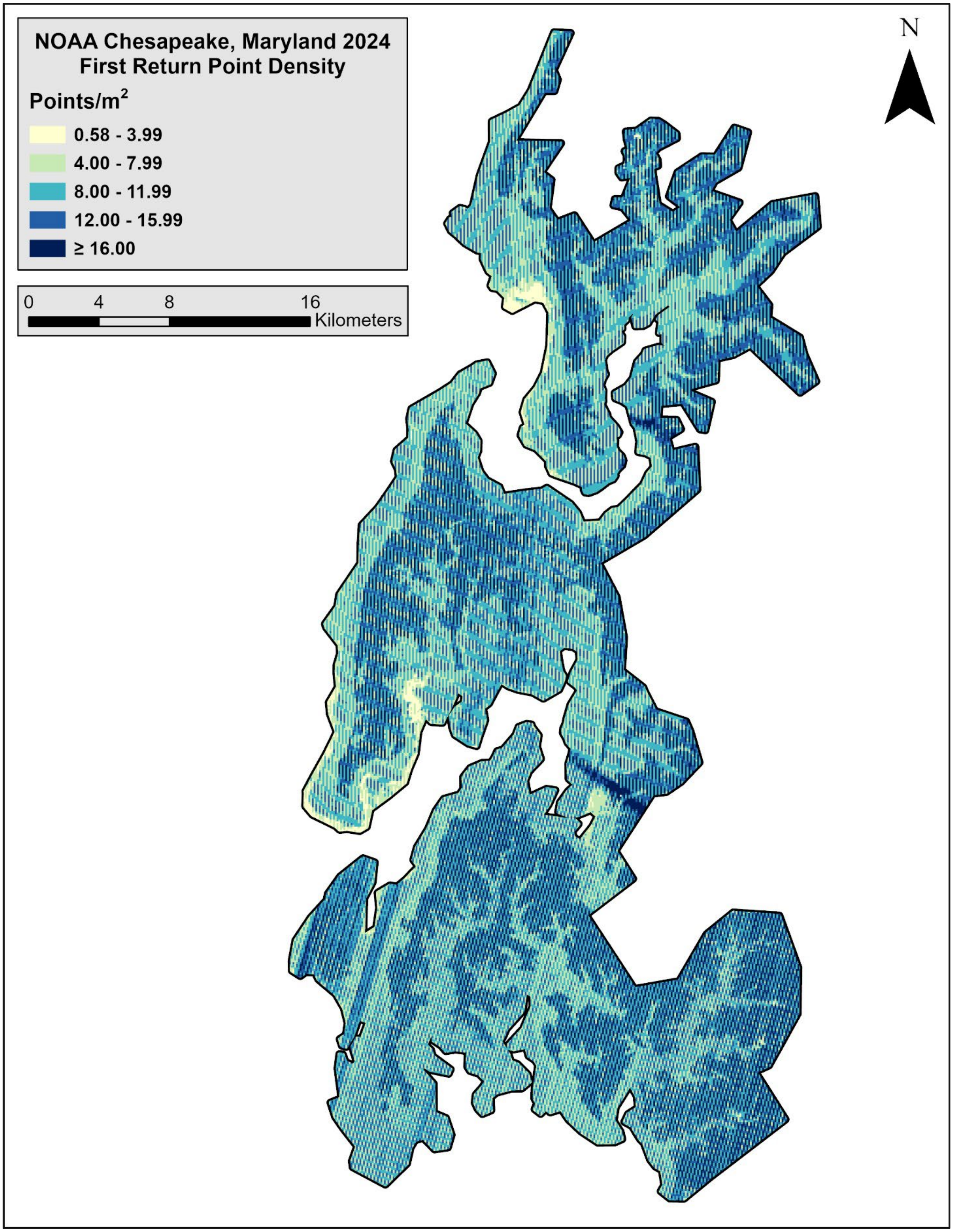

Figure 16: First return density map for the NOAA Chesapeake site (100 m x 100 m cells)

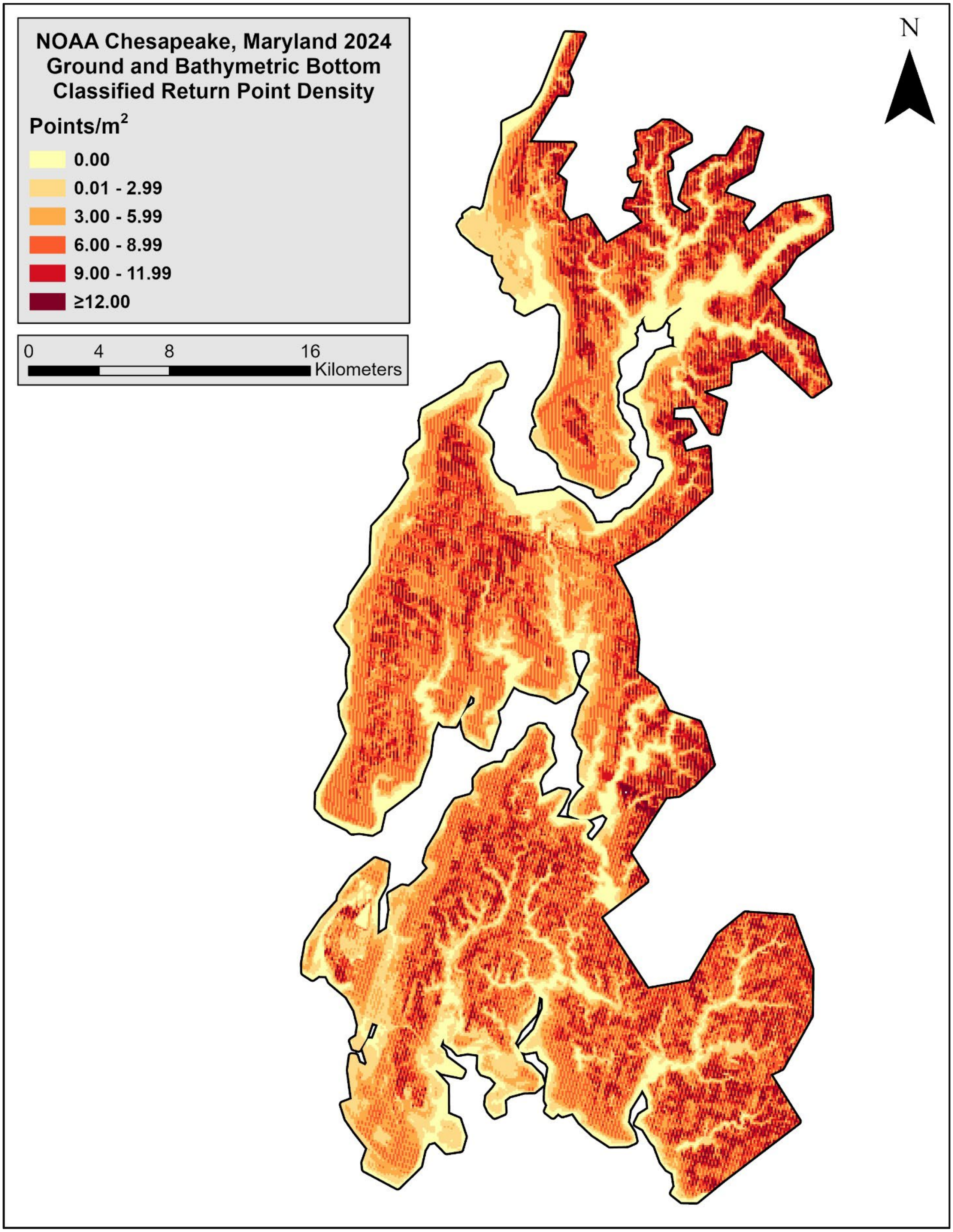

Figure 17: Ground and bathymetric bottom density map for the NOAA Chesapeake site (100 m x 100 m cells)

Lidar Accuracy Assessments

The accuracy of the lidar data collection can be described in terms of absolute accuracy (the consistency of the data with external data sources) and relative accuracy (the consistency of the dataset with itself). See Appendix A for further information on sources of error and operational measures used to improve relative accuracy.

Lidar Non-Vegetated Vertical Accuracy

Absolute accuracy was assessed using Non-Vegetated Vertical Accuracy (NVA) reporting designed to meet guidelines presented in the FGDC National Standard for Spatial Data Accuracy.[3] NVA compares known ground checkpoint data that were withheld from the calibration and post-processing of the lidar point cloud to the triangulated surface generated by the classified lidar point cloud as well as the derived gridded bare earth DEM. NVA is a measure of the accuracy of lidar point data in open areas where the lidar system has a high probability of measuring the ground surface and is evaluated at the 95% confidence interval (1.96 * RMSE), as shown in Table 12. This dataset was tested to meet ASPRS Positional Accuracy Standards for Digital Geospatial Data, Edition 2, Version 1 (2023) for a 10 cm RMSE Vertical Accuracy Class (Table 5).

The mean and standard deviation (sigma σ) of divergence of the ground surface model from ground checkpoint coordinates are also considered during accuracy assessment. These statistics assume the error for x, y, and z is normally distributed, and therefore the skew and kurtosis of distributions are also considered when evaluating error statistics to better evaluate the magnitude and distribution of the estimated error. For the NOAA Chesapeake survey, 35 ground checkpoints were withheld from the calibration and post processing of the lidar point cloud. The Non-Vegetated Vertical Accuracy (NVA) was found to be RMSE = 0.028 meters as compared to classified LAS, and RMSE = 0.028 meters as compared to the bare earth DEM (Figure 18 and Figure 19).

NV5 also assessed absolute accuracy using 30 ground control points. Although these points were used in the calibration and post-processing of the lidar point cloud, they still provide a good indication of the overall accuracy of the lidar dataset, and therefore have been provided in Table 12 and Figure 20.

[3] Federal Geographic Data Committee, ASPRS POSITIONAL ACCURACY STANDARDS FOR DIGITAL GEOSPATIAL DATA Edition 2, Version 1, 2023. https://aagsmo.org/wp-content/uploads/2023/03/ASPRS_PosAcc_Edition2_MainBody.pdf

Table 12: Absolute accuracy results

Parameter	NVA, as compared to classified LAS	NVA, as compared to bare earth DEM	Ground control points
Sample	35 points	35 points	30 points
95% Confidence (1.96*RMSE)	0.056 m	0.056 m	0.052 m
Average	-0.002 m	-0.002 m	0.001 m
Median	-0.004 m	-0.004 m	0.001 m
RMSE	0.028 m	0.028 m	0.026 m
Standard Deviation (1σ)	0.029 m	0.029 m	0.027 m

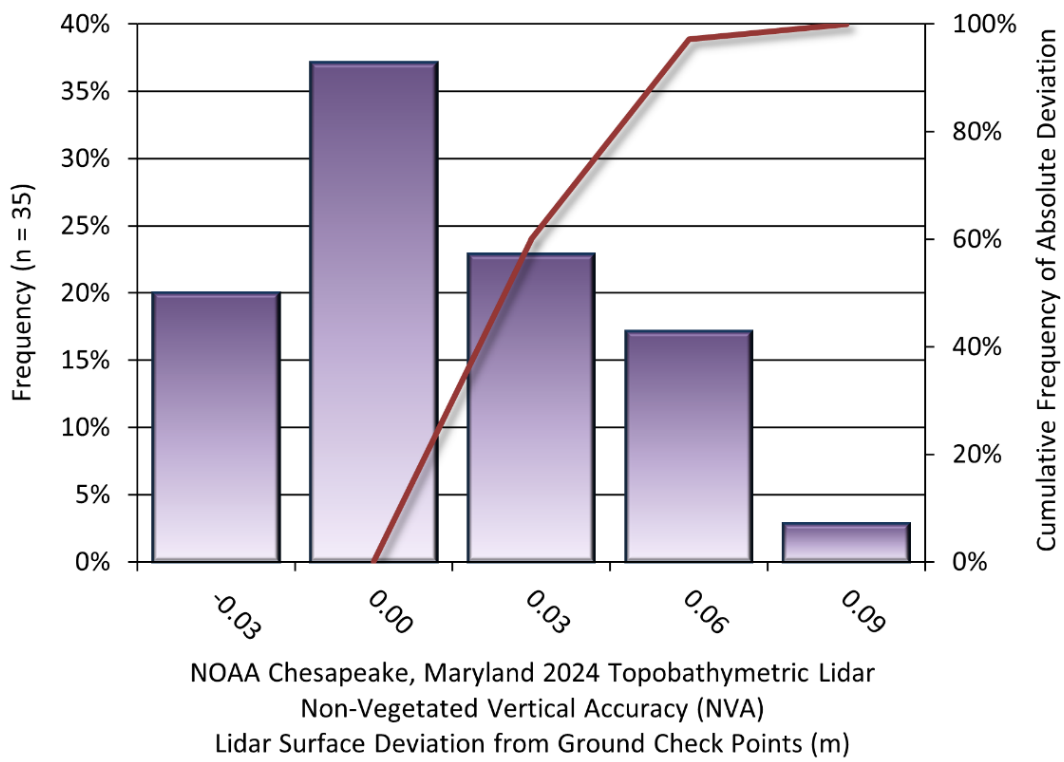

Figure 18: Frequency histogram for classified LAS deviation from ground checkpoint values

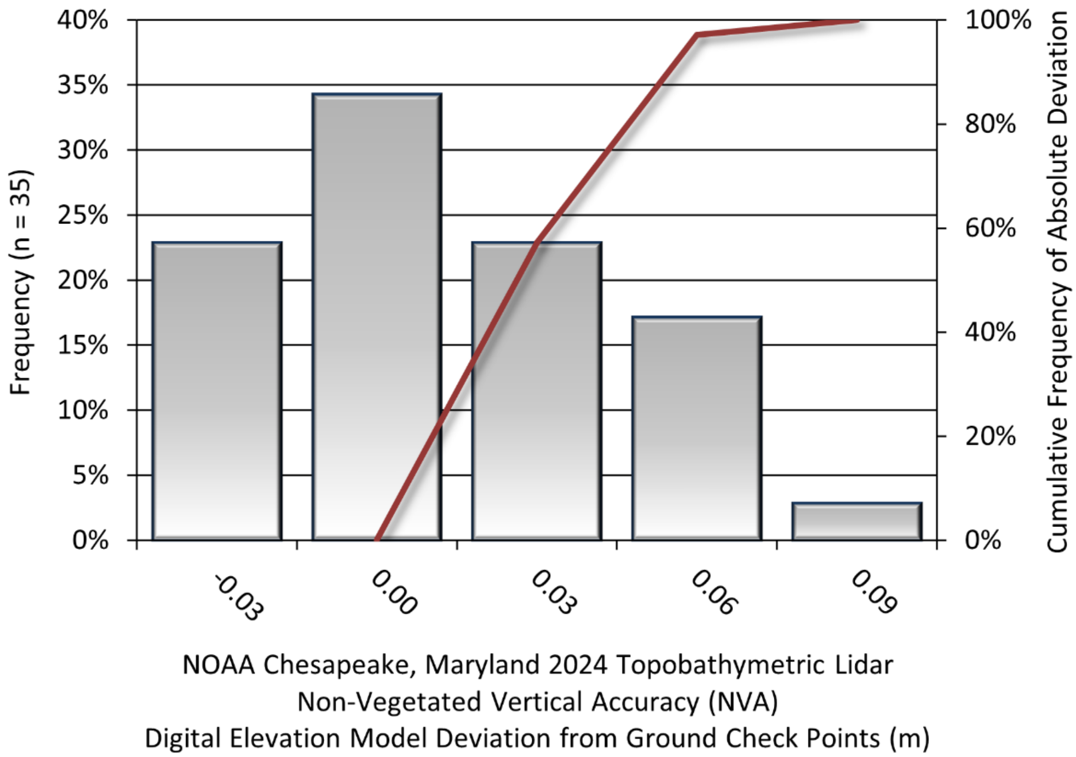

Figure 19: Frequency histogram for lidar bare earth DEM deviation from ground checkpoint values

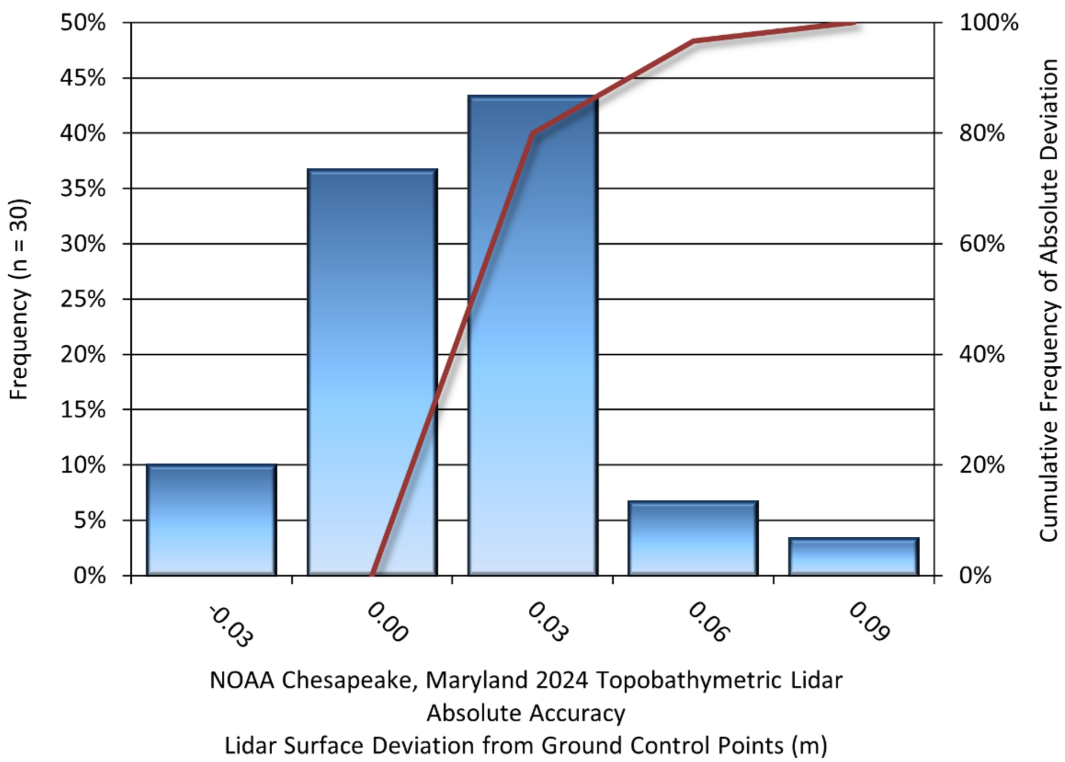

Figure 20: Frequency histogram for lidar surface deviation ground control point values

Lidar Vegetated Vertical Accuracies

NV5 also assessed vertical accuracy using Vegetated Vertical Accuracy (VVA) reporting. VVA compares known ground checkpoint data collected over vegetated surfaces using land class descriptions to the triangulated ground surface generated by the ground classified lidar points. Unlike in non-vegetated areas, the errors associated with data collected in vegetated areas cannot be assumed to approximate a normal distribution. This dataset was tested to meet ASPRS Positional Accuracy Standards for Digital Geospatial Data, Edition 2, Version 1 (2023) for a 10 cm RMSE Vertical Accuracy Class. The VVA was found to be RMSE = 0.102 meters as compared to the classified LAS, and RMSE = 0.104 meters as compared to the bare earth DEM.

Table 13: Vegetated Vertical Accuracy for the NOAA Chesapeake project

Parameter	VVA, as compared to classified LAS	VVA, as compared to bare earth DEM
Sample	35 points	35 points
95th Percentile	0.246 m	0.226 m
Average Dz	0.065 m	0.066 m
Median	0.049 m	0.046 m
RMSE	0.102 m	0.104 m
Standard Deviation (1σ)	0.079 m	0.082 m

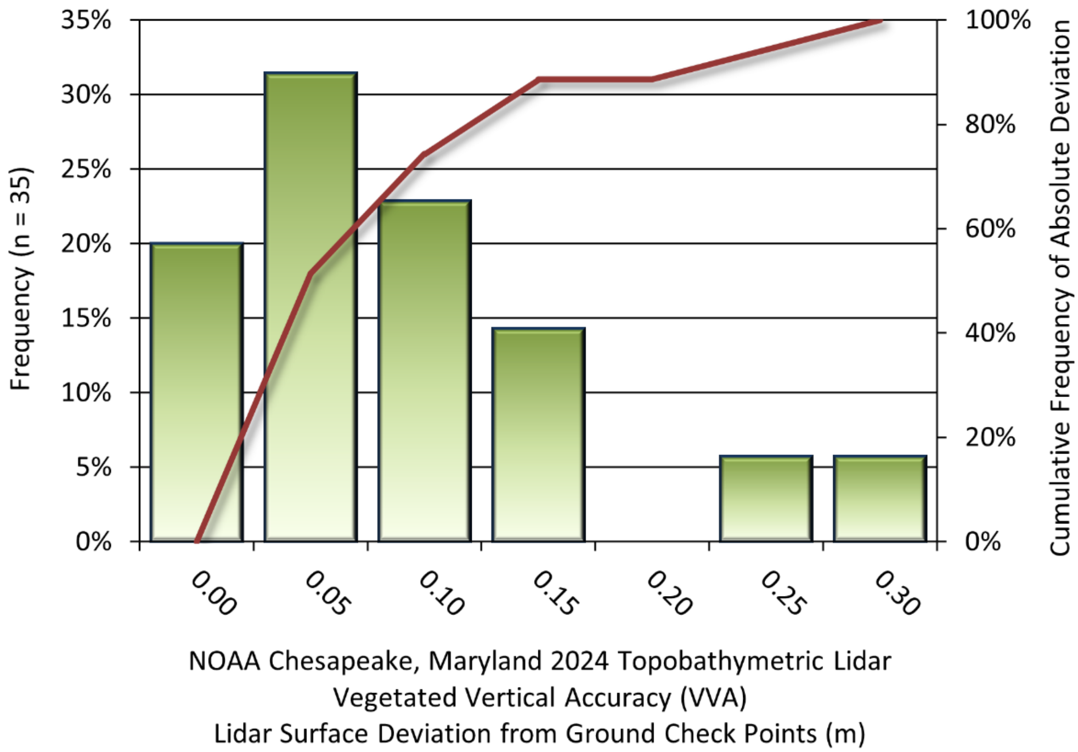

Figure 21: Frequency histogram for lidar surface deviation from all land cover class point values (VVA)

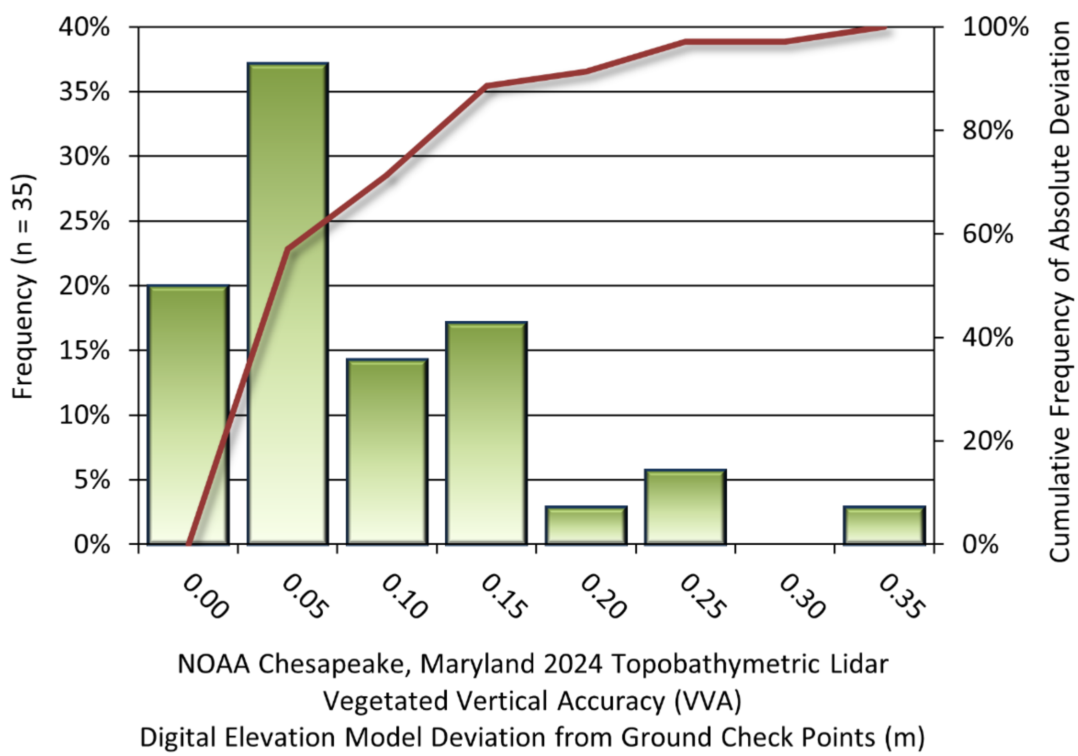

Figure 22: Frequency histogram for the lidar bare earth DEM deviation from vegetated checkpoint values (VVA)

Lidar Bathymetric Vertical Accuracies

Bathymetric (submerged) checkpoints were also collected in order to assess the submerged surface vertical accuracy. The Bathymetric Vertical Accuracy was found to be RMSE = 0.048 meters for 258 submerged points (Table 14 and Figure 23).

Table 14: Bathymetric Vertical Accuracy for the NOAA Chesapeake project

Parameter	Submerged Bathymetric Checkpoints
Sample	258 points
95th Percentile	0.094 m
Average Dz	0.006 m
Median	-0.002 m
RMSE	0.048 m
Standard Deviation (1σ)	0.047 m

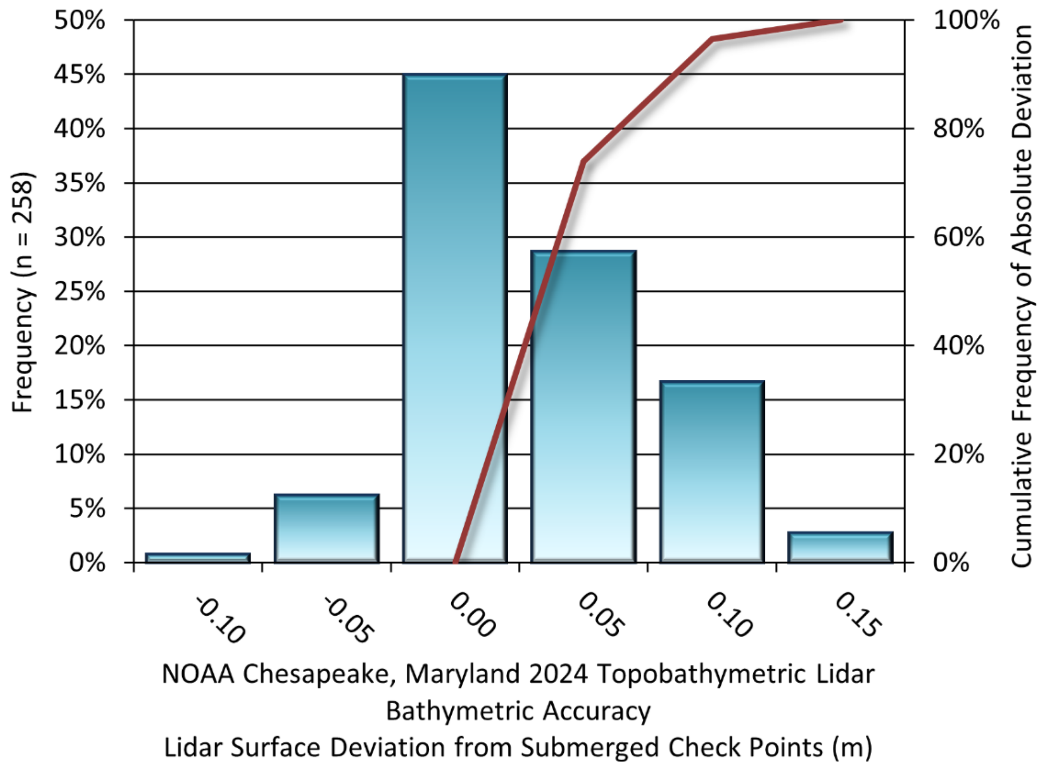

Figure 23: Frequency histogram for lidar surface deviation from submerged checkpoint values

Lidar Relative Vertical Accuracy

Relative vertical accuracy refers to the internal consistency of the dataset as a whole: the ability to place an object in the same location given multiple flightlines, GPS conditions, and aircraft attitudes. When the lidar system is well calibrated, the swath-to-swath vertical divergence is low (<0.10 meters). The relative vertical accuracy was computed by comparing the ground surface model of each individual flightline with its neighbors in overlapping regions. The average (mean) line to line relative vertical accuracy for the NOAA Chesapeake lidar project was 0.034 meters (Table 15, Figure 24).

Table 15: Relative accuracy results

Parameter	Relative accuracy
Sample	1019 flight line surfaces
Average	0.034 m
Median	0.041 m
RMSE	0.071 m
Standard Deviation (1σ)	0.049 m
1.96σ	0.096 m

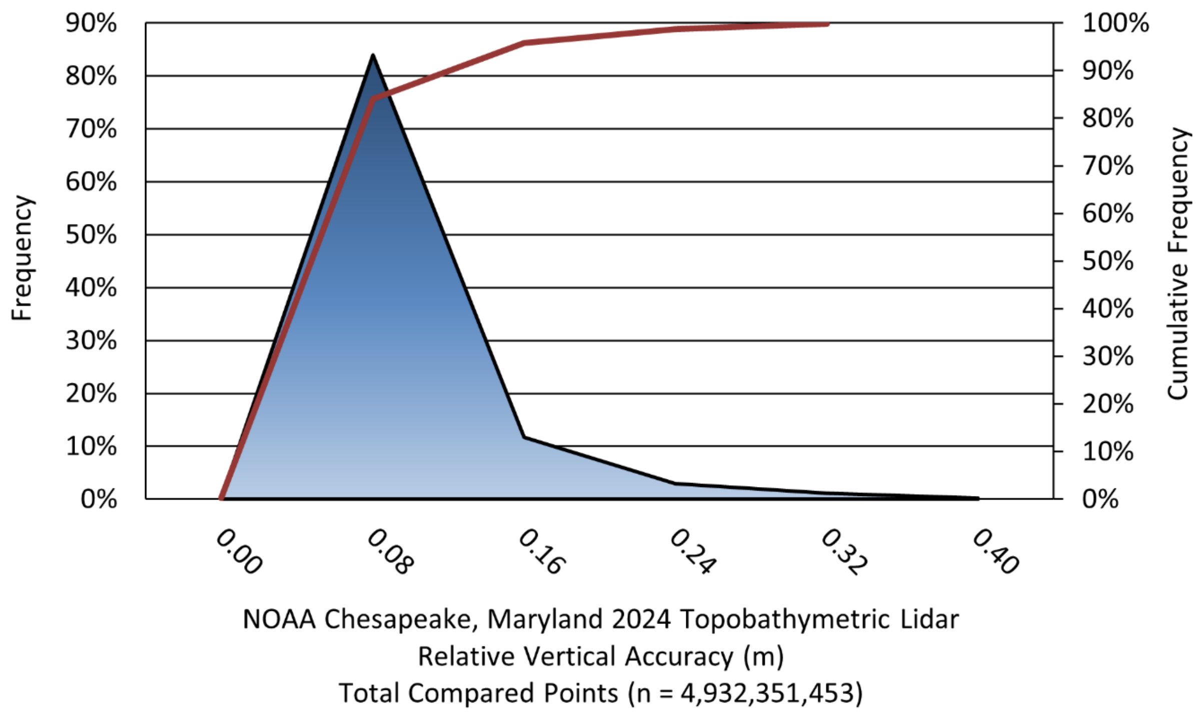

Figure 24: Frequency plot for relative vertical accuracy between flightlines

Lidar Horizontal Accuracy

Lidar horizontal accuracy is a function of Global Navigation Satellite System (GNSS) derived positional error, flying altitude, and inertial navigation system (INS) derived attitude error. The obtained RMSEr value is multiplied by a conversion factor of 1.7308 to yield the horizontal component of the National Standards for Spatial Data Accuracy (NSSDA) reporting standard where a theoretical point will fall within the obtained radius 95 percent of the time. Based on a flying altitude of 400 meters, an IMU error of 0.002 and 0.003 decimal degrees for roll/pitch and heading, respectively, and a GNSS positional error of 0.005 meters, this project was produced to meet a 0.029 meter $RMSE_H$ Horizontal Positional Accuracy Class for the CH4X sensor (Table 16). Based on a flying altitude of 400 meters, an IMU error of 0.002 and 0.004 decimal degrees for roll/pitch and heading, respectively, and a GNSS positional error of 0.008 meters, this project was produced to meet a 0.034 meter $RMSE_H$ Horizontal Positional Accuracy Class for the HE4X sensor (Table 16).

Table 16: Cumulative horizontal accuracy

Parameter	Chiroptera 400 m	HawkEye 400 m
IMU Error Roll and Pitch Combined	0.002 degrees	0.002 degrees
IMU Error Heading	0.003 degrees	0.004 degrees
GNSS Error	0.005 m	0.008 m
$RMSE_H$	0.029 m	0.034 m
ACC_r	0.049 m	0.059 m

NVS provided lidar services for the NOAA Chesapeake project as described in this report.

I, Alex McManus, have reviewed the attached report for completeness and hereby state that it is a complete and accurate report of this project.

Signed by:
Alex McManus
1D65E3271523487...

12/19/2025 | **2:44** PM PST

Alex McManus
Project
Manager
NVS

Surveyor's Certificate

I, Mark Edward Meade, being a Licensed Professional Land Surveyor in the state of Maryland, hereby certify to the best of my professional knowledge and belief that the survey methodologies and results shown on the attached report for the report titled NOAA Chesapeake, Maryland Shoreline Mapping Projects: MD2401-TB-C Technical Data Report, NOAA Contract 1305M220DNCNL0064, Task Order 1305M224F0373 dated December 19, 2025, were performed and obtained utilizing commonly acceptable survey standards, practices and procedures. The ground survey portion of this project was accomplished from November 4 to November 22, 2024. The aerial LiDAR was obtained from November 9 to November 19, 2024.

I have reviewed the accuracy statements as part of my oversight and found them to meet the National Standards for Spatial Accuracy (NSSDA) shown.

December 22, 2025

Mark E Meade

STATE OF MARYLAND
MARK EDWARD MEADE
21923
PROFESSIONAL LAND SURVEYOR

Mark Edward Meade
Professional Land Surveyor
Expires 10-25-26

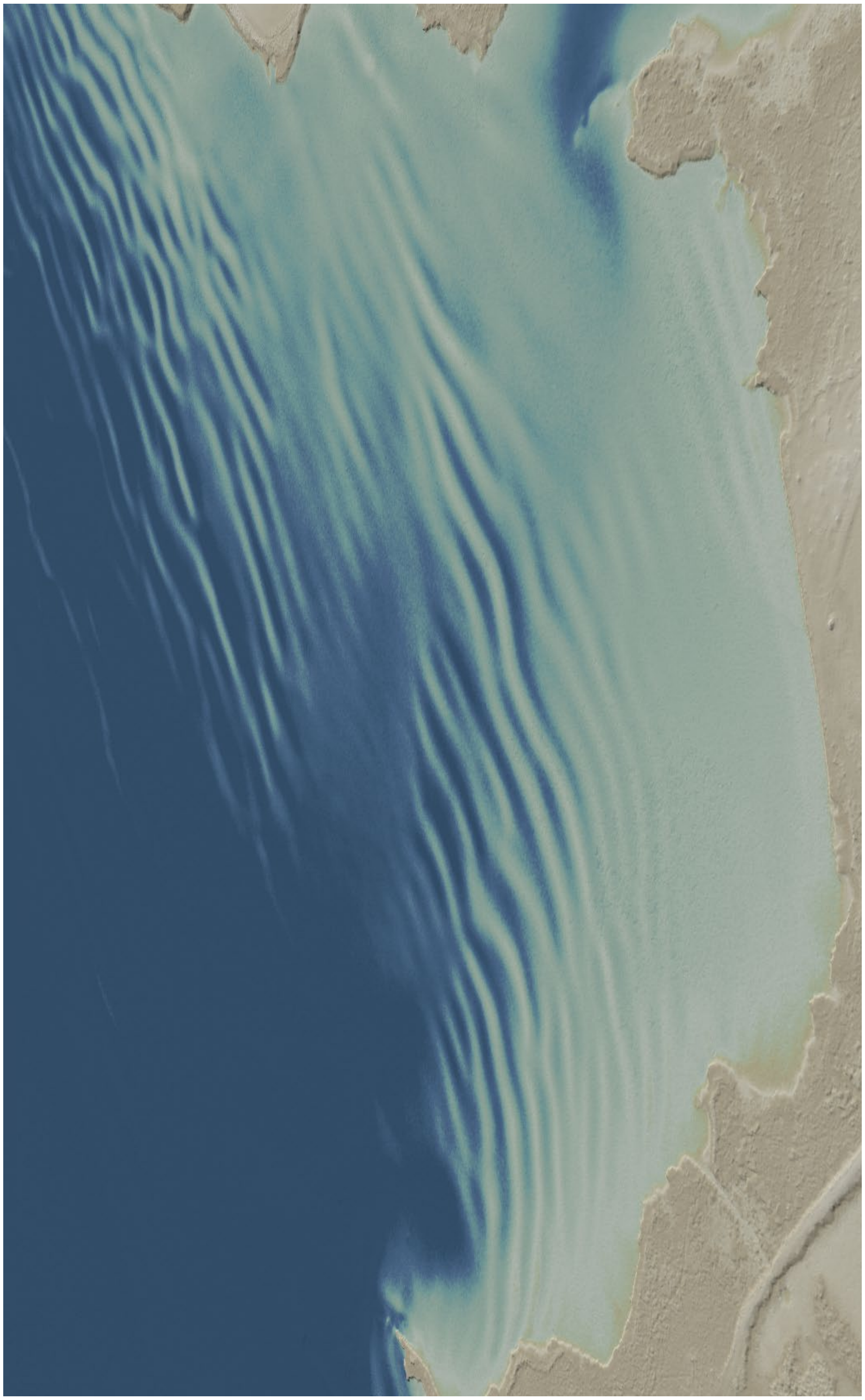

Figure 25: View looking north over Harbor Cove leading into the Chesapeake Bay. The image was created from the lidar bare earth model colored by elevation.

GLOSSARY

1-sigma (σ) Absolute Deviation: Value for which the data are within one standard deviation (approximately 68th percentile) of a normally distributed data set.

1.96 * RMSE Absolute Deviation: Value for which the data are within two standard deviations (approximately 95th percentile) of a normally distributed data set, based on the FGDC standards for Non-vegetated Vertical Accuracy (NVA) reporting.

Accuracy: The statistical comparison between known (surveyed) points and laser points. Typically measured as the standard deviation (sigma σ) and root mean square error (RMSE).

> **Absolute Accuracy:** The vertical accuracy of lidar data is described as the mean and standard deviation (sigma σ) of divergence of lidar point coordinates from ground survey point coordinates. To provide a sense of the model predictive power of the dataset, the root mean square error (RMSE) for vertical accuracy is also provided. These statistics assume the error distributions for x, y and z are normally distributed, and thus we also consider the skew and kurtosis of distributions when evaluating error statistics.
>
> **Relative Accuracy:** Relative accuracy refers to the internal consistency of the data set; i.e., the ability to place a laser point in the same location over multiple flight lines, GPS conditions and aircraft attitudes. Affected by system attitude offsets, scale and GPS/IMU drift, internal consistency is measured as the divergence between points from different flight lines within an overlapping area. Divergence is most apparent when flight lines are opposing. When the lidar system is well calibrated, the line-to-line divergence is low (<10 cm).
>
> **Root Mean Square Error (RMSE):** A statistic used to approximate the difference between real-world points and the lidar points. It is calculated by squaring all the values, then taking the average of the squares and taking the square root of the average.

Data Density: A common measure of lidar resolution, measured as points per square meter.

Digital Elevation Model (DEM): File or database made from surveyed points, containing elevation points over a contiguous area. Digital terrain models (DTM) and digital surface models (DSM) are types of DEMs. DTMs consist solely of the bare earth surface (ground points), while DSMs include information about all surfaces, including vegetation and man-made structures.

Intensity Values: The peak power ratio of the laser return to the emitted laser, calculated as a function of surface reflectivity.

Nadir: A single point or locus of points on the surface of the earth directly below a sensor as it progresses along its flight line.

Overlap: The area shared between flight lines, typically measured in percent. 100% overlap is essential to ensure complete coverage and reduce laser shadows.

Pulse Rate (PR): The rate at which laser pulses are emitted from the sensor; typically measured in thousands of pulses per second (kHz).

Pulse Returns: For every laser pulse emitted, the number of wave forms (i.e., echoes) reflected back to the sensor. Portions of the wave form that return first are the highest element in multi-tiered surfaces such as vegetation. Portions of the wave form that return last are the lowest element in multi-tiered surfaces.

Real-Time Kinematic (RTK) Survey: A type of surveying conducted with a GPS base station deployed over a known monument with a radio connection to a GPS rover. Both the base station and rover receive differential GPS data and the baseline correction is solved between the two. This type of ground survey is accurate to 1.5 cm or less.

Post-Processed Kinematic (PPK) Survey: GPS surveying is conducted with a GPS rover collecting concurrently with a GPS base station set up over a known monument. Differential corrections and precisions for the GNSS baselines are computed and applied after the fact during processing. This type of ground survey is accurate to 1.5 cm or less.

Scan Angle: The angle from nadir to the edge of the scan, measured in degrees. Laser point accuracy typically decreases as scan angles increase.

Native Lidar Density: The number of pulses emitted by the lidar system, commonly expressed as pulses per square meter.

Relative Accuracy Calibration Methodology:

Manual System Calibration: Calibration procedures for each mission require solving geometric relationships that relate measured swath-to-swath deviations to misalignments of system attitude parameters. Corrected scale, pitch, roll and heading offsets were calculated and applied to resolve misalignments. The raw divergence between lines was computed after the manual calibration was completed and reported for each survey area.

Automated Attitude Calibration: All data was tested and calibrated using TerraMatch automated sampling routines. Ground points were classified for each individual flight line and used for line-to-line testing. System misalignment offsets (pitch, roll and heading) and scale were solved for each individual mission and applied to respective mission datasets. The data from each mission were then blended when imported together to form the entire area of interest.

Automated Z Calibration: Ground points per line were used to calculate the vertical divergence between lines caused by vertical GPS drift. Automated Z calibration was the final step employed for relative accuracy calibration.

Lidar accuracy error sources and solutions:

Source	Type	Post Processing Solution
Long Base Lines	GPS	None
Poor Satellite Constellation	GPS	None
Poor Antenna Visibility	GPS	Reduce Visibility Mask
Poor System Calibration	System	Recalibrate IMU and sensor offsets/settings
Inaccurate System	System	None
Poor Laser Timing	Laser Noise	None
Poor Laser Reception	Laser Noise	None
Poor Laser Power	Laser Noise	None
Irregular Laser Shape	Laser Noise	None

Operational measures taken to improve relative accuracy:

Focus Laser Power at narrow beam footprint: A laser return must be received by the system above a power threshold to accurately record a measurement. The strength of the laser return (i.e., intensity) is a function of laser emission power, laser footprint, flight altitude and the reflectivity of the target. While surface reflectivity cannot be controlled, laser power can be increased and low flight altitudes can be maintained.

Reduced Scan Angle: Edge-of-scan data can become inaccurate. The scan angle was reduced to a maximum of ±20° to ±21° for the green and NIR lasers, respectively, from nadir, creating a narrow swath width and greatly reducing laser shadows from trees and buildings.

Quality GPS: Flights took place during optimal GPS conditions (e.g., 6 or more satellites and PDOP [Position Dilution of Precision] less than 3.0). Before each flight, the PDOP was determined for the survey day.

Ground Survey: Ground survey point accuracy (<1.5 cm RMSE) occurs during optimal PDOP ranges and targets a minimal baseline distance of 4 miles between GPS rover and base. Robust statistics are, in part, a function of sample size (n) and distribution. Ground survey points are distributed to the extent possible throughout multiple flight lines and across the survey area.

50% Side-Lap (100% Overlap): Overlapping areas are optimized for relative accuracy testing. Laser shadowing is minimized to help increase target acquisition from multiple scan angles. Ideally, with a 50% side-lap, the nadir portion of one flight line coincides with the swath edge portion of overlapping flight lines. A minimum of 50% side-lap with terrain-followed acquisition prevents data gaps.

Opposing Flight Lines: All overlapping flight lines have opposing directions. Pitch, roll and heading errors are amplified by a factor of two relative to the adjacent flight line(s), making misalignments easier to detect and resolve.